NAVAL POSTGRADUATE SCHOOL

Monterey, California

THESIS

EFFECTS OF FUEL ADDITIVES ON PLUME OPACITY OF A SUB-SCALE TURBOJET TEST CELL WITH A RAMJET TYPE DUMP-COMBUSTOR

by

Thomas Richard Darnell

December 1979

Thesis Advisor: D. W. Netzer

Approved for public release; distribution unlimited.

SECURITY CLASSIFICATION OF THIS PAGE (When Data Entered)

REPORT DOCUMENTATION PAGE	READ INSTRUCTIONS BEFORE COMPLETING FORM
1. REPORT NUMBER	2. GOVT ACCESSION NO. AD-A084516
	3. RECIPIENT'S CATALOG NUMBER (9)
4. TITLE (and Subtitle) (6) Effects of Fuel Additives on Plume Opacity of a Sub-Scale Turbojet Test Cell with a Ramjet Type Dump-Combustor.	5. TYPE OF REPORT & PERIOD COVERED Master's Thesis; December 1979
	6. PERFORMING ORG. REPORT NUMBER
7. AUTHOR(s) (10) Thomas Richard Darnell	8. CONTRACT OR GRANT NUMBER(s) N6237679WR00014
9. PERFORMING ORGANIZATION NAME AND ADDRESS Naval Postgraduate School Monterey, California 93940	10. PROGRAM ELEMENT, PROJECT, TASK AREA & WORK UNIT NUMBERS
11. CONTROLLING OFFICE NAME AND ADDRESS Naval Air Propulsion Center Trenton, New Jersey 08628	(11) 12. REPORT DATE December 1979
	13. NUMBER OF PAGES 76
14. MONITORING AGENCY NAME & ADDRESS(if different from Controlling Office) Naval Postgraduate School Monterey, California 93940	15. SECURITY CLASS. (of this report) Unclassified
	15a. DECLASSIFICATION/DOWNGRADING SCHEDULE

16. DISTRIBUTION STATEMENT (of this Report)

Approved for public release; distribution unlimited.

17. DISTRIBUTION STATEMENT (of the abstract entered in Block 20, if different from Report)

18. SUPPLEMENTARY NOTES

19. KEY WORDS (Continue on reverse side if necessary and identify by block number)

Turbojet
Test Cell
Pollution

20. ABSTRACT (Continue on reverse side if necessary and identify by block number)

An initial investigation was conducted into the effects of metallic based fuel additives on smoke reduction in turbojet test cells.

Experiments were conducted on a one-eighth scale turbojet test cell with a ramjet type dump-combustor. Measurements of particle sizes and concentrations were made using light transmittance at two wavelengths. Particulate samples were

DD FORM 1 JAN 73 1473 EDITION OF 1 NOV 65 IS OBSOLETE
S/N 0102-014-6601
(Page 1)

SECURITY CLASSIFICATION OF THIS PAGE (When Data Entered)

collected and examined with a scanning electron microscope.

Increased combustor temperatures and fuel additives appeared to affect particle size and concentration primarily downstream of the engine exhaust. Recommendations are made for experimental technique improvements which are required to improve the quality of the data.

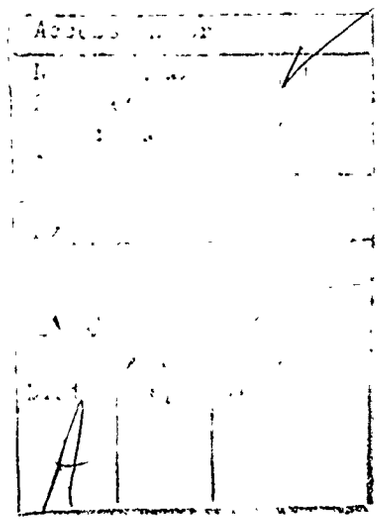

Approved for public release; distribution unlimited.

Effects of Fuel Additives on Plume Opacity of a Sub-Scale Turbojet Test Cell with a Ramjet Type Dump-Combustor

by

Thomas Richard Darnell
Lieutenant Commander, United States Navy
B.S., University of Illinois, 1968

Submitted in partial fulfillment of the
requirements for the degree of

MASTER OF SCIENCE IN AERONAUTICAL ENGINEERING

from the

NAVAL POSTGRADUATE SCHOOL
December 1979

Author 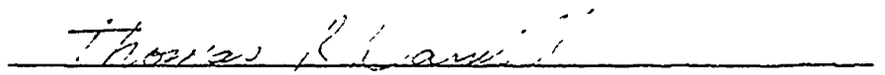

Approved by: 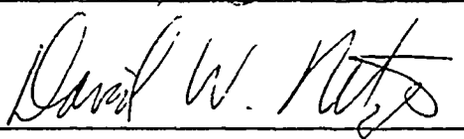
Thesis Advisor

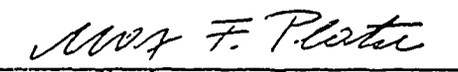
Chairman, Department of Aeronautics

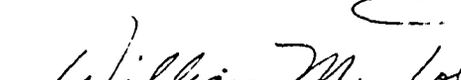
Dean of Science and Engineering

ABSTRACT

An initial investigation was conducted into the effects of metallic based fuel additives on smoke reduction in turbojet test cells.

Experiments were conducted on a one-eighth scale turbojet test cell with a ramjet type dump-combustor. Measurements of particle sizes and concentrations were made using light transmittance at two wavelengths. Particulate samples were collected and examined with a scanning electron microscope.

Increased combustor temperatures and fuel additives appeared to affect particle size and concentration primarily downstream of the engine exhaust. Recommendations are made for experimental technique improvements which are required to improve the quality of the data.

TABLE OF CONTENTS

LIST OF TABLES

LIST OF FIGURES

ACKNOWLEDGEMENT

The author wishes to extend his gratitude and appreciation to the many people of the Department of Aeronautics who provided welcome advice and support in this project. Bob Besel's friendly staff of skilled technicians and craftsmen aided in solving many seemingly insurmountable problems. In particular, the author thanks Ted Dunton for his ability to make anything work, Pat Hickey for his months of meticulous work which made the project possible, and Jim Hammer for the many extra hours after hours he put in while the test cell was operating.

A very special thanks must go to a tremendous thesis advisor, Associate Professor David W. Netzer. It was indeed a pleasure to have had the opportunity to work with such a devoted and talented educator and scientist.

Finally, sincerest appreciation is extended to the author's family, his wife Connie and two daughters Melissa and Erica, for their patience and understanding throughout his studies at the Naval Postgraduate School.

I. INTRODUCTION

Jet engine test cells are stationary structures which enable the jet engine to be operated under controlled, static conditions. Such facilities are required for engine development, post-maintenance and post-overhaul turn-ups. They permit instrumentation for troubleshooting and qualifying engines in a manner that could not be done were the engine installed in its intended airframe. Thus, test cells are a vital part of the logistics and safety programs for both military and commercial aviation.

Like all fuel-burning devices, jet engines expel emissions. In light of the 1970 amendments to the Clean Air Act and the standards established by the Environmental Protection Agency (EPA), engine manufacturers, commercial aviation and the military establishment have placed emphasis on the reduction and/or elimination of harmful emissions generated by jet engines. There is considerable difficulty in determining what the acceptable levels of emission from the jet engine combustion process should be and whether or not the standards are attainable. The EPA issued emission standards which apply to jet engines installed in commercial and private aircraft in 1973. Military aircraft are not subject to these standards. In addition, standards specifically applicable to jet engine test cells had not been formulated. Since jet engines are thought of as being associated

with aircraft, a mobile device, it was believed that U.S. Navy jet engine test cells would not be subject to local ambient air quality restrictions. However, due to the amendment to the Clean Air Act in 1977 [Ref. 1] and recent court decisions, test cells may be classified as stationary sources of pollution and subject to regional and community pollution control boards. Hence, regulations might vary significantly from facility to facility. As a case in point, the Navy is currently in litigation over allegations that it does not meet local standards in the San Diego Air Pollution Control District and the Bay Area Pollution Control District [Ref. 2]. Thus, there are the potential problems of jurisdiction and the meeting of different regulations in different geographical locations.

The exhaust of the gas turbine engine is made up primarily of large volumes of nitrogen, oxygen, carbon dioxide and water vapor. Within this, in relatively small quantities, are particulates, oxides of nitrogen (NO_x), sulfur dioxide (SO_x), unburned hydrocarbons (UHC) and carbon monoxide (CO). The quantities and proportions of these emissions can vary greatly depending on the engine type and the operating level of the engine. This is particularly true for military engines due to the very wide operating ranges required of them. For example, a fighter aircraft requires engines that operate at power settings from idle through afterburner as opposed to a commercial engine which effectively operates at only one or two power settings.

The jet engine per se has not been a major contributor of pollution to any particular region. The emissions from aircraft engines have been estimated to be of the order of less than 3% of the overall urban pollution problem [Ref. 3]. This, along with the fact that controlling jet engine emissions is a very complex problem, has resulted in a relatively slow start toward developing abatement systems and anti-pollution technology for installed engines.

One long-term means of controlling emissions is through major engine redesign. Thus, emission control may be built into new engine technology. The development of smokeless combustors is an example. Such work is costly in time and money but represents strides toward acceptable long-term solutions. The redesign of certain commercial aircraft engines has resulted in some reduction in the output of hydrocarbons, carbon monoxide and smoke emissions. However, the control of oxides of nitrogen is not considered practicable with current technology [Ref. 1]. Some of the newly developed commercial engine technology is directly transferable to military engines. New technology application may be limited, however, by the degree to which the performance of the engines differs, i.e., high-performance military engines as opposed to commercial engines [Ref. 1]. Thus, for many current inventory engines in service, technology changes may prove impractical due to performance degradation and economic considerations. Since the emissions expelled by a test cell are a function of the engine being operated, short-term solutions to test cell emission control are needed.

As stated earlier, the purpose of a test cell is to provide a facility in which an engine may be operated throughout its entire operating spectrum so that performance deficiencies may be detected prior to installation in an aircraft. Since the engine operating performance is highly dependent on the inlet conditions of the air, the cell must be carefully designed so as to provide flow and thermal fields free of distortions at the engine face. It must also be designed so that exhaust gases are not reingested. Figure 1 illustrates the general layout of a typical test cell. The inlet and exhaust structures are primarily designed for noise abatement. The augmentor tube serves as a jet pump and ensures that air flow occurs from front to aft over the engine and that the pressure differential across the engine is kept to a minimum. It also pumps relatively cool air down the augmentor to mix with the hot engine exhaust gases in order to limit structural temperatures. The consideration of any modifications to the test cell for the purpose of pollution abatement must be done in such a manner as to not alter the design characteristics of the cell. To do so would not allow an accurate assessment of engine performance and would negate the usefulness of the test cell.

In the public view, the most offensive pollutants discharged by jet engines are noise and smoke since they are so readily observed. Since a test cell absorbs much of the noise generated from within, smoke becomes the focal point of

immediate concern. Thus, a significant effort has gone into reducing the opacity of the test cell exhaust plume.

Opacity as defined by the EPA is the degree to which emissions reduce the transmission of light and obscure the view of an object in the background [Ref. 4]. The apparent reduction of light is due to absorption and scattering of light by particulate matter in the exhaust. Opacity is related to the transmittance of light beams through the exhaust gas by:

$$\% \text{ OPACITY} = 100\% - \% \text{ TRANSMITTANCE.}$$

Several techniques have been used as a measure or description of opacity. A method used by some pollution control districts to specify regulations on opacity is to use what is known as Ringelmann Number (RN). RN's range from 0 to 5 with 0 representing 0% opacity and 5 representing 100% opacity. A typical regulation might specify a maximum opacity of Ringelmann Number 1, i.e., 20% opacity. The RN is determined by a trained human observer. The difficulty with this method is that it is subjective and not continuous. Another method of measuring opacity is with a commercial optical transmissometer. The device is designed to measure the attenuation of a light beam transmitted through the exhaust stream. Its advantages over the human observer are that the readings are objective, consistent, provide a permanent and continuous record, and can be calibrated to read opacity directly.

In the case of a jet engine exhaust, light transmittance is blocked by the presence of particulates which are by weight about 96% carbon [Ref. 3]. The formation of the gaseous emissions and the carbon particulates take place in the combustor of the turbine engine. Figure 2 illustrates a typical jet engine combustor. In the primary burn zone, the fuel-air mixture is often inhomogeneous, with regions of fuel-rich mixtures. In these regions, liquid hydrocarbons can be broken down to produce soot/particulates. As the carbon leaves the primary burn zone and moves downstream, more oxygen becomes available and burning may occur on the surface of the carbon particles. The maximum allowable temperature on the engine structure and turbine blades is limited, so cooler air must be mixed with the hot gases to prevent engine damage. This quenching lowers the gas temperature to the point where carbon will no longer burn and the remaining carbon particles are forced out the exhaust.

The exact process by which particulates are formed in the turbojet combustion process is not entirely understood. McDonald [Ref. 5] suggested that the process begins with the accretion of carbon nuclei in the flame zone followed by aggregation via coagulation creating "carbon particles" due to quenching beyond the flame zone. McDonald went on to suggest that "soot particles" are formed by further aggregation prior to the exhaust gases leaving the tailpipe. When the engine is installed in a test cell, changes may continue to occur in the augmentor tube and/or the stack. This

possibility must be considered when examining means of reducing test cell plume opacity.

The size of the particulates in question is not well documented. One study found that particulates ranged in size from 0.01 to 0.5 microns [Ref. 6], while others report particulate diameters of 0.05 to 0.1 microns with occasional increases to 0.125 microns [Ref. 3]. It has also been reported that particulates will agglomerate into clusters having dimensions of 0.6 to 0.8 microns [Ref. 3]. Data from Ref. 6 illustrates that particulate sizes and concentrations will vary depending on engine type, power setting and distance from the exhaust nozzle to where the sample is taken.

One technique used to reduce the plume opacity of jet engine test cells is to use fuel additives. Many such additives have been developed and at least eighteen have been evaluated by the Naval Air Propulsion Center for possible use in Navy facilities [Ref. 7]. Some of the more effective additives are metallic based and may cause engine performance degradation due to deposits building up on the combustor walls and on turbine blades. The exact process by which fuel additives reduce smoke opacity is not well understood. Robson, Kesten, and Lessard [Ref. 3] suggest that additives are probably effective because they act as oxidation catalysts which speed up oxygen transfer to the hydrocarbon molecule or because they may lower the ignition temperature of the soot and limit the growth size of the particles. Pagni and Hughes [Ref. 8] suggest that additives serve as surface

catalysts of soot oxidation or act as an inhibitive agent of the carbon particle agglomeration mechanism. Pagni and Hughes also report that it is not clear whether the metal-based additives actually reduce total carbon particulate mass emission or simply redistribute particle sizes to reduce their visibility while forming metal oxides. Howard and Kausch [Ref. 9] have suggested three different mechanisms for soot removal depending upon the type of metallic additive: (a) production of ions which either decrease the amount of soot formed or produce smaller sizes which are more readily consumed, (b) production of hydroxyl radicals which remove soot from the flame, and (c) acceleration of the soot oxidation rate in the secondary flame zone. Manganese and iron-based additives are proposed to function by the latter mechanism.

Reference 7 reports that of the eighteen additives evaluated, ferrocene ($FeC_{10}H_{12}$) was found to be the most effective overall additive. By adding ferrocene in proper porportions to the engine fuel, test cell exhaust opacity was reduced from as high as 55% opacity to below 20% opacity [Ref. 10]. It also appeared that ferrocene did not have any detrimental effects on the environment or short-term adverse effects on the engine. Tests have also shown it to be relatively non-toxic. Long-term effects are still under investigation.

It is obvious that plume opacity is related to particulate size and concentration, but what is not clear is how these

properties are altered by the test cell and by the use of fuel additives. Particulates may be altered within the combustor as discussed above. In addition, when the particulates leave the combustor, they are subjected to the effects of dilution from bypass air in the engine (if present), dilution in the augmentor tube, and mixing and cooling in the stack prior to exiting to the atmosphere.

It is the overall purpose of the investigation at the Naval Postgraduate School to study the effects of engine operating conditions (flow rates, fuel/air ratio and temperature), test cell design (augmentation ratio, etc.) and fuel additives on the emitted particles from a turbojet test cell. This study was the initial investigation of this program. Specifically, the effects of two metallic additives (ferrocene and DGT-2) and combustor operating conditions on the concentration and size of particulate matter at the engine and stack exhausts were studied. Mean particulate size and concentration were measured by means of a multiple-frequency light transmission technique at the engine exhaust and at the test cell exit plane. The opacity of the test cell plume was also measured by the use of a commercial transmissometer in order to relate the readings of this often-used device to quantitative particulate data. Particulate samples were collected at both the engine exhaust and test cell exit and examined with the aid of an electron microscope in order to provide additional quantitative data on particulate sizes.

II. EXPERIMENTAL APPARATUS

A. SUB-SCALE TURBOJET TEST CELL

The one-eighth scale turbojet test cell described in Refs. 11 and 12 was used to carry out this investigation. The test cell, shown in Figure 3, is a scale model of a Naval Air Station, Alameda test cell. Figure 4 illustrates the basic plumbing and Figure 5 shows data sensor locations on the test cell. Air was drawn into the test cell through a horizontal inlet with a square bellmouth and a flow straightening section. The test section was enclosed by hinged plexiglas sides to allow easy access and visual monitoring during operation. The augmentor tube exited the cell through a removable wall. Its downstream end was attached to a deflector-plate-equipped vertical exhaust stack. The stack was mounted on a wheel/rail arrangement which allowed translation of the stack/augmentor assembly.

High-pressure air was provided to the externally mounted combustor from a large-volume positive displacement compressor. The combustor exhaust was routed to the nozzle in the test section where it was mixed with bypass air. The bypass air was supplied from an Allis-Chalmers, twelve-stage axial flow compressor. The engine inlet was simulated with a six-inch pipe drawing air through a six-inch bellmouth. An ejector was employed to provide the suction air flow rate. Pneumatically activated servo control valves were installed in each of the four air lines so that air mass flow could be remotely

regulated. The "engine inlet" suction air was adjusted so that it approximated the total mass flow of the combustor and bypass air.

B. COMBUSTOR

The combustor utilized for the test was a ramjet type dump-combustor. The combustor is illustrated in Figure 6 and described in Ref. 13. The combustion chamber was designed to operate at pressures of nine atmospheres or greater. The sudden expansion chamber provided good flame stabilization. It was ignited with an oxygen-ethylene torch which was located in the flame stabilizing recirculation zone. The primary and secondary air flows were supplied by a positive displacement compressor with a line pressure of approximately 150 PSIA. A typical total combustor air mass flow rate was about 0.5 LBM/SEC. By varying the primary fuel/air ratio and secondary air flow, the exhaust temperature and particulate concentration (i.e., opacity) could be altered. A secondary fuel injection location was available but not used. The combustion pressure was decreased to approximately two atmospheres by the use of two sonic nozzles. The combustor was water cooled to protect the chamber walls and lower the total temperature.

C. FUEL CONTROL SYSTEM

The portable fuel supply system, illustrated in Figure 7, consisted of two regulated, nitrogen pressurized tanks, with an associated remote control panel (Figure 8). From the

control panel the fuel flow rate was controlled and combustor temperature monitored. One fuel tank contained JP-4 jet fuel while the other contained a mixture of JP-4 and the fuel additive under investigation. Both fuel tanks were pressurized by the same nitrogen source and controlled by a common regulator, thus ensuring that both fuel sources had equal upstream pressures. The plumbing was arranged so that by properly opening and closing a pair of identical electrical solenoid valves, either tank could feed fuel to the primary fuel manifold of the combustor. From each tank, the pressurized fuel was filtered, passed through a separate electrical solenoid valve, through a common cavitating venturi and then directed to the primary fuel manifold. The function of the cavitating venturi was to permit the adjustment of fuel flow rate by variation of the upstream pressure only. The fuel flow rate versus upstream pressure was pre-calibrated for the cavitating venturi used [Ref. 13] and is shown in Figure 9.

D. INSTRUMENTATION AND DATA COLLECTION SYSTEM

The test cell was fully instrumented for the calculation of air flow rates, cell temperatures and pressures, and the augmentation ratio. Figure 5 shows the locations of pressure and temperature sensors.

Flow rates in the six-inch suction line, three-inch bypass line, and the combustor primary and secondary air source lines were measured using ASME type flow orifices. Pressure taps

in the test cell allowed monitoring of pressure at the cell entrance and at the engine inlet and exhaust planes. Eleven pressure taps along the top of the augmentor tube and six copper-constantan thermocouples were used to monitor pressure and temperature in the augmentor tube. The velocity profile in the augmentor was measured with a pitot rake consisting of seven equally spaced small diameter total pressure tubes. The rake was fixed at approximately four inches from the stack end of the augmentor in a vertical position. From the velocity profile, augmentor mass flow rate was calculated and used to determine the augmentation ratio.

All of the pressure lines were terminated in a 48-port, automatic-stepping scanivalve with a 500-PSI differential pressure transducer. The leads from each thermocouple were routed through an ice bath reference to an HP-3495A scanner.

The fully automatic data acquisition system was centered about an HP-21 MX computer system. Thermocouple and pressure transducer readings were automatically read in via two HP-3495A scanners and an HP-3455A digital voltmeter. The data processing program was based on ASME flow calculations [Ref. 14]. Figures 10 and 11 are copies of typical output data sheets.

E. TRANSMISSOMETER

The commercial transmissometer fixed at the exit of the test cell stack, Figure 12, was provided by the Naval Air Rework Facility, North Island, California. The model used

was a Leeds and Northrup model 6597. This transmissometer consists of an incandescent light source, a light detector, and a signal conditioner/display unit. The signal conditioner/display unit is shown in Figure 8. The light source and detector were mounted on opposite sides of the stack. (See Figure 12.) The output reads directly as percent opacity. Calibration data reported in Ref. 4 indicated that output is linear. Reference 4 also provides additional information on this transmissometer.

F. LASERS AND DETECTORS

The technique used to measure the particulate concentration and mean size is based on measuring the total amount of light removed from a beam passing through the exhaust. The loss of light is due to both absorption and scattering by the particulates. The transmission of light through an aerosol of particles is given by Bouguer's Law [Ref. 15]:

$$T = EXP\ (-\gamma L)$$

where T is the transmittance, L is the distance through the aerosol, and γ is the turbidity. For a polydisperse system of particles, Ref. 16 reports the turbidity to be:

$$\gamma = \frac{3}{2} \frac{\overline{Q} C_m}{D_{32} \rho}$$

where C_m is the mass concentration of particles, ρ is the density of an individual particle, D_{32} is the volume to surface mean diameter, and $\bar{Q}$ is the average extinction coefficient. Cashdollar also reports [Ref. 16] that values of $\bar{Q}$ are not significantly affected by the exact shape of the size distribution, but primarily by the mean diameter D_{32}. Using Mie scattering theory, the average extinction coefficient $\bar{Q}$ is calculated as a function of particle size distribution, wavelength of the light beam, complex refractive index of the particles, and the mean particle diameter. Cashdollar provided a Fortran program to the Naval Postgraduate School which can be used to calculate the extinction coefficient as a function of the above variables. Figure 13 shows how the extinction coefficient varies with the mean particle diameter for three wavelengths (4880, 5145, and 6328 Angstroms). These curves were generated for a log normal particle size distribution with a standard deviation of $\sigma = 1.5$ and a refractive index of 1.8 - .3i.

From Bouguer's Law [Ref. 16] the ratio of the logarithms of the measured transmission at any two wavelengths is equal to the ratio of the computed average extinction coefficients:

$$\frac{\text{Ln } T_{\lambda_1}}{\text{Ln } T_{\lambda_2}} = \frac{\bar{Q}_{\lambda_1}}{\bar{Q}_{\lambda_2}} \quad .$$

Curves from which average particle size can be found as a function of the $\bar{Q}$ ratios are shown in Figure 14.

With the average particle size and extinction coefficient known and given a particle density, the mass concentration can be calculated from:

$$C_m = - \frac{2}{3} \frac{\rho D_{32}}{\bar{Q}_\lambda L} \text{Ln } T_\lambda \ .$$

As noted by Cashdollar [Ref. 16], the use of three wavelengths provides a redundancy over most of the particle size range. If the three measured log transmission ratios do not yield the same approximate average particle diameter, then the particle size distribution and/or the refractive index may not be correct. For this study, wavelengths of 4880Å, 5145Å, and 6328Å were available. It was expected that the $\bar{Q}$ ratio $\bar{Q}(6328Å)/\bar{Q}(4880Å)$ would be most accurate because of the larger spread between the wavelengths. The wavelength 5145Å was too close to the other two wavelenths to obtain meaningful redundant data. Therefore, only two wavelengths were used and redundant data were not available to determine the exact index of refraction and size distribution. Since a prior knowledge of the refractive index and size distribution were not available, only representative values for particle diameter and concentration were obtainable. Data obtained from the SEM were used to obtain an approximate mean particle diameter. With this, an estimated value for size distribution and refractive index were obtained.

The light source used by Cashdollar [Ref. 16] was a halogen-filled tungsten-filament lamp, placed directly across the test section from the detector. In this experiment, it was desired to direct the beam across two different test sections and to have a remotely located light source. Since the light had to travel over a distance of several feet where it would be subject to atmospheric attenuation, it was decided to utilize lasers for the light sources. Lasers were also selected so that a determination could be made as to the adequacy of the light source for the transmission technique involved. If the laser source proved adequate, the technique might be extended for use in locations such as airfields to study exhaust particulates from aircraft while taking off or landing, without interfering with operations.

An eight-milliwatt helium-neon laser was used for the 6328Å (red) source and a five-watt argon-ion laser was used for the 4880Å (blue) source. The argon-ion laser could also provide a 5145Å (green) source, but as mentioned above, was not used. The lasers were located in a structure adjacent to the test cell to protect them from weather. Figure 15 illustrates the beam path. The beam to the stack exhaust traveled about 26 feet and the beam to the nozzle exhaust traveled about 26.5 feet before entering the respective test section. Outside the test section, the beams were contained in tubing to minimize interference from test cell soot fallout and atmospheric dust.

Each detector unit had a 1/4-inch inside diameter, 12-inch long tube at its entrance to eliminate any significant forward light scattering. Figure 16 illustrates the arrangement of photo diodes and filters in the detector units. Note that the detector is normally covered so that only light entering the tube is measured. Each of these photo diodes was covered by a narrow pass filter of wavelength 6328Å, 5145Å, or 4880Å, as appropriate. The output of each photo diode was input to an operational amplifier, providing linearity between light intensity and voltage output. Output from each detector was continuously recorded on a strip chart.

G. PARTICULATE COLLECTION

Particulates were collected by their impact on a 3/8-inch diameter aluminum pedestal which was used as a specimen mount in the electron microscope. To collect particles exiting the nozzle, the pedestal was placed directly in the nozzle plume 4.5 inches downstream from the nozzle (Figure 17). Before the test cell was turned up, the pedestal was placed on its mount in the augmentor tube facing downstream. During the run the pedestal was moved into the plume and rotated 180 degrees to face the nozzle. It was left for only a moment to avoid particulate buildup, and then turned downstream.

Particulate collection at the stack exhaust required a slightly different arrangement. The stack exhaust velocity was low relative to that of the nozzle exit and the particulate

concentration was lower due to augmented air flow. Thus, the small particles tended to track the air stream rather than impact on the blunt pedestal in the flow field. A small skirt was placed around the pedestal to slow the air and funnel more particles to the pedestal. Figure 18 illustrates the arrangement. Figure 12 illustrates the collector in place at the stack exhaust.

III. EXPERIMENTAL PROCEDURE

As indicated by Ref. 10, the concentration of fuel additives required to reduce opacity varies with engine type. To determine the concentration required for the combustor used for this study, it was first experimentally determined what fuel/air ratio would yield an opacity between 30% and 50%. The opacity was measured with the commercial transmissometer. After the high opacity was reached, the fuel additive under study was added to the fuel in increasing proportions until a significant reduction in opacity was achieved. This established a baseline from which the study was conducted.

The first step of collecting data was to place particulate collection pedestals on their mounts in the augmentor tube just downstream of the nozzle. (See Figure 17.) The pedestals were turned downstream until samples were desired. The test section of the test cell was then secured and the laser detector moved into position.

Since the optical system was very sensitive, a complete checkout and realignment of the laser beams and detectors was required before each day's operations. This generally involved making small corrections to the optical mirrors and/or beam splitters and beam power adjustments by placing neutral density filters in the beam. The desired detector output, with no particulates present, was 5 to 10 volts for both of the wavelengths.

It was found that small vibrations transmitted through the concrete slab on which the laser and optics were mounted caused a 50 to 70 Hz fluctuation of about ±.5 volts in the output. Attempts to dampen out the vibrations were not made due to the major redesign and reconstruction effort involved. An attempt to filter the output signal resulted in an unacceptably slow response time; thus the filter was not used.

After alignment, calibrated neutral density filters were inserted in the beams to certify that linear outputs were obtained.

The commercial transmissometer was rigidly mounted to the stack and did not require alignment. Reference 4 reported transmissometer output to be linear. This was not reconfirmed.

The mass flow rates through the combustor, nozzle bypass and inlet suction lines were set from a control panel remotely located at the computer terminal. After each flow adjustment was made a computer run was made to check the flow rates. This process was repeated until the desired flow rate was achieved in each line. The nozzle bypass and inlet suction lines could be adjusted independent of other flow rates. However, the two air lines to the combustor received air from the same source and these flow rates were dependent on each other. Thus, adjusting the combustor primary and secondary air flow rates to desired proportions was sometimes tedious and time-consuming. It was also found that the total primary and secondary combustor air flow could not exceed approximately

0.6 LBM/SEC without decreasing the supply pressure. To properly simulate the flow within the test cell, the inlet air was set to equal the sum of the total combustor and nozzle bypass flow rates.

The desired fuel flow rate was set by pressurizing the two fuel tanks to the necessary level. Figure 9 illustrates the venturi pressure which must be maintained to achieve a particular fuel flow rate. After the tank pressure was established, either tank could be selected to feed fuel to the combustor.

With all air flow rates set and fuel flow off, the oxygen-ethylene torch was ignited by a spark ignitor. The torch was given a few moments to stabilize before JP-4 (without additives) was injected into the combustor. After ignition, the torch was extinguished. When the combustor exit temperature and opacity were steady, a computer run was made to obtain flow rates and other test cell parameters. Particulate samples were taken at the stack and nozzle exhausts. The temperature of the combustor coolant water and nozzle exhaust were visually noted and recorded. Combustor exit temperature was recorded on a strip chart.

Initially, after all readings were made and the strip chart recordings appeared stable, the JP-4 (without fuel additives) was shut off and simultaneously the JP-4 with the fuel additive was turned on. After several tests, it was found that it was necessary to run at higher temperatures than initially anticipated. Since the combustor exhaust

pipe was not water cooled, run time was limited at the higher temperature to approximately 30 seconds. Therefore, the procedure was changed. After all data were collected for JP-4 (without fuel additives), the fuel was shut off without changing any other settings. After the combustor exhaust pipe cooled, the combustor was reignited using JP-4 with the fuel additive. Again, after opacity and temperature readings were stable, particulate samples were taken, a computer run made and visual data recorded.

The particulate samples were taken to the Hopkins Marine Laboratory, Monterey, California, where they were examined with a scanning electron microscope (SEM). Of interest was the relative mean size of particles collected at the nozzle to those collected at the stack exhaust. No attempt was made to determine the size distribution.

IV. RESULTS AND DISCUSSION

A. INTRODUCTION

The data obtained in this study are summarized in Tables I through IV. Tables I and II present the primary data collected. After review of the initial results, secondary data were collected in an attempt to substantiate primary data and fill in missing information. The secondary data are shown in Tables III and IV. The runs are numbered consecutively from 1 through 15 for identification and discussion purposes. Note that "DESCRIPTION" identifies the fuel and additive (if any) used and applies to run pairs (except in the case of run number 15). Significant changes occurred in transmittance as the combustor exit temperature (t_1) exceeded approximately 1350°F. Therefore, two temperature regions warrant discussion, i.e., greater than and less than 1350°F. For ease of discussion, those runs where t_1 was less than 1350°F will be referred to as "low temperature" and those greater than 1350°F as "high temperature" runs.

Figure 19 illustrates typical output of the transmissometer and the temperature of the gases exiting the combustor (t_1). The fuel was JP-4 with approximately 0.2% ferrocene by weight. Figure 20 illustrates typical transmittance output from the laser detector unit mounted on the stack. Both Figure 19 and Figure 20 are outputs from run numbers 3 and 4 of Tables I and II.

Figures 21 through 27 are photographs of collected stack particles as viewed with a scanning electron microscope (SEM). The scale for each figure is printed on the photograph as 5U or 0.5U with a line representing that length over it. The U represents microns. Figures 21 and 22 are photographs taken of a sample obtained with JP-4 without additives during a low-temperature run. Figure 23 was obtained for a test without additives but at a higher combustor exhaust temperature. Figures 24, 25 and 26 are photographs of samples obtained using JP-4 with 0.2% ferrocene. These samples were taken during a low-temperature run. Figures 27 and 28 are photographs of samples obtained using JP-4 with 0.2% DGT-2 during a high-temperature run. All of these photographs are typical of what was found on the collectors. Approximate ranges of average particulate diameters [(maximum diameter + minimum diameter)/2] are listed in Table II. All the samples collected at the engine exhaust were unsatisfactory. The surfaces of the aluminum pedestals appeared to be highly eroded and individual particles were indistinguishable.

Since the mechanism by which the additive reduces opacity is of importance, a brief comparison of the ramjet type dump-combustor used in this study to a turbojet combustor is needed. Fuel atomization in the dump-combustor was achieved by driving the fuel through eight 0.010-inch holes located circumferencially in the pipe wall upstream of the combustion chamber. (See Figure 6.) This was done to achieve a good

primary fuel/air mixture. This is a slightly different technique from that used in the typical turbojet (see Figure 2), but the difference should not significantly alter the manner in which the formation of carbon particles is initiated nor the mechanism by which an additive operates within the primary combustion zone. In the dump-combustor there appeared to be good flame stability and a distinct primary combustion zone as is found in a turbojet. Of significant difference is the rapid air quench in the dump-combustor as opposed to the gradual dilution in the turbojet. Additive effects in the dilution zone could be significantly different, depending upon the residence time required for the dominant mechanism of the additive. Recall that Howard and Kausch [Ref. 9] have suggested that the mechanism by which manganese and iron-based additives reduce soot is by accelerating the soot oxidation rate in the secondary (dilution) flame zone. The two additives used in this investigation were ferrocene and DGT-2. Ferrocene is iron-based and DGT-2 is a manganese-based additive. Gradual cooling/particle growth should be similar in the dump-combustor tailpipe and sub-scale test cell to that in an actual turbojet and test cell. During the experiments, the nozzle was operated at high subsonic to just choked conditions.

A combustor operating point had to be found which provided a significant plume opacity when operating without an additive. This would provide a reference from which to compare

the effects of an additive. It was found that the primary fuel-to-air ratio (F/A_p) had to be near stoichiometric or fuel-rich to achieve a plume opacity of 30 to 50% as measured by the transmissometer. Any significant increase in F/A_p on the rich side had little effect on opacity. Combustor exhaust gas temperature had to be monitored closely due to the uncooled combustor exhaust pipe. If the exhaust temperature exceeded approximately 1400°F, the exhaust pipe would take on a bright red glow. Run time at high temperatures was therefore limited to avoid serious structural degradation of the system. Combustor secondary air flow was used to regulate the exhaust temperature, i.e., F/A_{p+s} was controlled to limit t_1.

The effective mixture ratio of ferrocene to JP-4 is a function of the engine type/combustor design [Ref. 10]. In an attempt to find the proper mixture ratio for the dump-combustor, mixtures of 0.05% to 0.4% by weight of ferrocene were tried. F/A_p and F/A_{p+s} were set such that t_1 did not exceed approximately 1300°F to avoid the hardware problem in the exhaust pipe. The maximum reduction in opacity achieved was about 14%. It was also found that the reduction was a non-linear function of mixture ratio, i.e., opacity reductions of 6%, then 14%, then 6% were obtained as the % ferrocene was increased. Subsequent testing revealed that ferrocene significantly reduced opacity only when the combustor was operated with an exhaust temperature exceeding approximately 1350°F. These higher temperatures were achieved by increasing

the fuel flow rate while maintaining fixed primary and secondary combustor air flow rates.

Since combustor exhaust gas temperature appeared to be a major factor in plume opacity, the effects of temperature with and without fuel additives will be examined first.

B. TEMPERATURE EFFECTS ON JP-4 WITHOUT ADDITIVES

From the data of runs 1, 2, 7 and 8, it was noted that the temperature increased from less than 1300°F to greater than 1400°F. The transmittance of white light (transmissometer) at the stack increased about 28%. Correspondingly, transmittances of red and blue light at the stack increased by about 30% while the transmittances at the engine increased very little (4% to 13%). Since changes in percent transmittance of the stack exhaust were significantly greater than at the engine exhaust, it is reasonable to conclude that temperature changes in the burner affected agglomeration downstream of the engine. It should be noted, however, than run 2 was conducted on a different day with a different fuel fill. This may have affected the data. Further tests need to be conducted to verify these results.

By using Figure 14 and the experimentally determined ratio of extinction coefficients at the stack exhaust for the low-temperature run, the mean particle diameters were determined to be either 0.11μ or 0.16μ (μ represents microns). These were only representative diameter values since the exact value of standard deviation of the particle size distribution

and the refractive index of the particles were not known and could not be determined with only two wavelengths. A third wavelength would provide the redundant information necessary to determine these parameters. In the absence of better information, Figure 14 was used because it provided the best fit of available theoretical curves to the experimentally obtainable $\bar{Q}_r/\bar{Q}_b$ ratios. The $\bar{Q}$ ratio for the stack on the high temperature run was smaller than for the lower temperature run and fell below the minimum value of the curve on Figure 14. This implied that the mean diameter shifted toward the minimum point of the curve. However, what was not clear was on which side of the curve the data belonged. If on the left, the data implied that the particles were becoming larger and conversely, if on the right the particles were becoming smaller as the exhaust temperature was increased. SEM data for run 1 (Figure 22) indicated that the range of particle diameters was between 0.11μ and 0.15μ. This was between the values determined from the light measurements and did not conclusively indicate which side of the curve was most probable. However, SEM data clearly indicated that the particle diameters in run 1 were greater than those of run 2 (Figure 23). This implied that the right side of the curve (Figure 14) was probably correct as discussed above. If this data is presumed valid, then it can be concluded that the hotter exhaust gases decreased the particle size. Since the ratio $\bar{Q}/D_{32}$ does not vary significantly (Figure 13), the

transmittance data also indicates that the concentration decreased.

To validate these results, a third wavelength is required so that the correct relationship between the $\bar{Q}$ ratios and mean particle diameter can be determined. Also needed is improved transmittance and SEM data at the engine exhaust. It should also be noted that the particulate samples were not collected iso-kinetically, but rather by an impact process which could generate differences between the size distribution of particles collected/observed and that which actually existed in the exhaust gases.

C. TEMPERATURE EFFECTS ON JP-4 WITH FERROCENE

From the data for runs 3, 4, 9 and 10 it was noted that as the temperature was increased the transmittance of the white light source (transmissometer) increased (14% in runs 3 and 4, 42% in runs 9 and 10). However, transmittance of the red and blue sources at the stack each decreased by about 10%. The red transmittance at the engine increased only slightly as it did without ferrocene. The stack effect appears to be inconsistent; that is the discrete wavelengths decreased in transmittance and the white source increased in transmittance. It was also noted that the effects were much smaller than without ferrocene.

Again, from the $\bar{Q}$ ratios, representative values of particle diameter were determined from Figure 14 and are presented in Table II. For the low-temperature run the diameters were

0.08μ or 0.20μ. Since the $\bar{Q}$ ratio remained essentially unchanged as temperature was increased, it is unlikely that the particle size was affected, i.e., the mean particle diameter was either about 0.08μ or 0.20μ. SEM data (Figures 25 and 26) indicated a fairly even distribution of particle diameters from 0.09μ to 0.14μ. The SEM data did not clarify which side of the theoretical curve was most likely because of the wide spread in observed diameters. However, since the low-temperature data should have been similar to the corresponding run without additives (run 1) it might be reasonably concluded that the larger diameter is more probable.

From Bouguer's Law, assuming particle density was constant, it was evident that if the mean diameter did not change [and therefore $\bar{Q}$ did not change (see figure 13)], then concentration must have changed if there was to be a change in transmittance. Since the transmittance of both the red and blue sources decreased, this implied that concentration increased. Again, however, this is inconsistent with both the red transmittance at the engine exhaust and the white light transmittance at the stack which both increased.

Due to this inconsistency, no conclusion could be drawn without further data. However, one consideration which might be examined is the effect of iron oxide on scattering, i.e., is it possible that discrete wavelengths are affected differently than a wide wavelength spectrum by the simultaneous presence of metallic oxide and soot particles?

D. TEMPERATURE EFFECTS ON JP-4 WITH DGT-2

It should be noted that the high temperature run (run 6) was only marginally hotter and, therefore, the changes in transmittance may not be well pronounced, making comparison difficult. The transmittance of the white source again increased (14%) as the temperature increased. At the stack the red and blue transmittance remained virtually unchanged while at the engine, both the red and blue transmittance increased very slightly. This data appeared to be consistent with that obtained with ferrocene.

Since the $\bar{Q}$ ratios did remain essentially unchanged with the temperature change, the mean particle diameter probably was unchanged by the temperature variation. Again using Figure 14, the possible mean particle diameter was about 0.08μ or 0.19μ. The SEM data (Figure 28) indicated a range of particle diameters of 0.12μ to 0.15μ. This tended to indicate that the right side of the curve was preferred which is consistent with the case without additives. Note that the trends in data for DGT-2 and ferrocene were very similar, i.e., transmittance in red and blue decreased or remained unchanged at the stack and increased at the engine, transmittance in white light increased at the stack, and the mean particle diameters remained virtually unchanged when the exhaust temperature changed. However, as with ferrocene, no definite conclusions can be made at this point.

It should be noted that in all three of the above cases the transmittance at the engine went up with temperature in

very similar manners. It would appear then that the effects of temperature were consistently occurring downstream of the engine exhaust.

To examine the effects of adding an additive to the fuel, four comparisons were made: JP-4 with and without ferrocene and DGT-2 for both low and high temperature runs.

E. FERROCENE EFFECTS ON OPACITY DURING LOW-TEMPERATURE OPERATION

The data for runs 1 and 3 were extracted for the same exhaust gas temperature. The flow rates for the two runs were also very similar. Going from JP-4 (run 1) to JP-4 with ferrocene (run 3), the transmittances increased for each light source. The white light transmittance increased by about 11%, the stack red increased by 7% and stack blue increased by 26%. The engine red increased by 3% and engine blue increased by 10%. The transmittance changes at the engine were significantly less than those at the stack. This again implied that significant changes occurred downstream of the engine, in this case as a result of fuel additive.

The $\bar{Q}$ ratios increased slightly which would imply that the particle size increased slightly if it were assumed that the right side of the curve in Figure 14 applied as was established in the previous discussion. The SEM data, however, indicated that there was a negligible change in particle size at the stack. If, in fact, stack particle diameter was not significantly changed, then the increased transmittance

would be caused by a decrease in particle concentration, i.e., less mass flow.

F. DGT-2 EFFECTS ON OPACITY DURING LOW-TEMPERATURE OPERATION

The data for runs 1 and 5 were compared at similar temperatures; however, the flow rates between the two runs were different making comparison difficult. Note from Table I that the total augmentor air flow rate for run 5 was significantly lower than for run 1. This lower dilution effect would tend to drive transmittance down which appeared to be what happened. In each case, the transmittance from run 5 was slightly lower than for run 1. Further data will need to be collected before any comment can be made on the effects of DGT-2.

G. FERROCENE EFFECTS ON OPACITY DURING HIGH-TEMPERATURE OPERATION

Comparison of run 2 to run 4 showed that the transmittance of red and blue light at the stack decreased with ferrocene. The white transmittance remained about the same. There also was no significant change in transmittance at the engine. The secondary data set (runs 8 and 10) indicated a 13% increase in transmittance of white light when ferrocene was used.

The $\bar{Q}$ ratio between runs 2 and 4 indicated a significant increase in particle diameter (assuming the right side of the curve in Figure 14). But this, with the recorded decrease in red and blue transmittance would imply that concentration

must have increased significantly. This contradicted the fact that the white light transmittance did not decrease.

This inconsistency again brought out the need for obtaining comparative data on the same day with identical fuel lots. Too many contradictions occurred to draw any definite conclusions from this data. However, runs 8 and 10 were made under well controlled conditions and showed a significant decrease in opacity with the use of ferrocene at the 0.2% level. This was also evident in earlier runs when the ferrocene was added during one continuous run.

H. DGT-2 EFFECTS ON OPACITY DURING HIGH-TEMPERATURE OPERATION

As before, there was a dilution problem between the runs which needed to be compared. No data were available for a meaningful comparison to be made.

V. CONCLUSIONS AND RECOMMENDATIONS

This initial investigation resulted in some findings of a preliminary nature on the effects of metallic based additives on smoke opacity. There was evidence that additive effects were similar to those resulting from an increased exhaust gas temperature, i.e., major changes in opacity took place downstream of the engine. Some indication was also present that additives may also affect particle concentration. The degree of change, however, was not clear from available data. The very small changes in light transmittance at the engine exhaust for different test conditions may indicate that the particle sizes were too small to be adequately detected with the optical technique which was utilized.

It was found that small changes in experimental conditions and data accuracy had a strong impact on the results and subsequent calculations for particle diameter and concentration. Therefore, experimental improvements are required in order to obtain better quantitative data. It is recommended that the following changes be made to the experimental procedures and/or apparatus:

A. A three-wavelength system should be used (vice two) so that the correct standard deviation and refractive index of the particles can be determined. Separate light sources should be used for the stack and engine exhaust. The light source should be mounted directly across from the detector to minimize external interference effects on beam intensity. The light sources should be powered by regulated power supplies to ensure a constant beam intensity output.

B. At the engine exhaust, the light beam should be contained up to the nozzle and again immediately after the nozzle to avoid any possible effects on transmittance by air flow in the test cell.

C. The light source should be a white light (vice lasers) to eliminate the complication of beam alignment. This would also provide a wider spread in the choice of wavelengths.

D. The linearity of the transmissometer should be verified and the output calibrated.

E. An improved particle collection technique is required at the engine exhaust. The pedestals should be machined from stainless steel (vice aluminum) to resist the high temperatures encountered. The collection technique should be such that the samples can be taken and removed from the test cell during that portion of the run in which samples are desired.

F. A cooled combustor exhaust pipe is required to permit hotter runs for longer periods of time so data can stabilize at the higher temperatures and to allow switching fuel sources without shutdown.

RUN NR.	DESCRIPTION	$\dot{m}_f$	$\dot{m}_p$	$\dot{m}_s$	$\dot{m}_{e_{AIR}}$	$\dot{m}_{t_{AIR}}$	AUG. RATIO	F/A_p	F/A_{p+s}	P_{tp}
1	JP-4 W/O	.0145	.212	.203	1.30	6.47	4.0	.068	.035	27.7
2*	ADDITIVES	.0147	.198	.179	1.29	6.58	4.1	.074	.039	26.9
3	JP-4 W/ .2%	.0145	.207	.216	1.33	6.41	3.8	.070	.034	27.6
4	FERROCENE	.0150	.207	.216	1.33	6.41	3.8	.072	.035	27.6
5	JP-4 W/ .2%	.0151	.217	.184	1.30	5.44	3.2	.070	.038	27.5
6	DGT-2	.0157	.217	.184	1.30	5.44	3.2	.072	.039	27.5

LEGEND

$\dot{m}_f$: fuel flow rate (lbm/sec)

$\dot{m}_p$: primary combustor air flow rate (lbm/sec)

$\dot{m}_s$: secondary combustor air flow rate (lbm/sec)

$\dot{m}_{e_{AIR}}$: total engine air flow rate (lbm/sec)

$\dot{m}_{t_{AIR}}$: total air flow rate in augmentor tube (lbm/sec)

AUG. RATIO : augmentation ratio

F/A_p : fuel to primary air ratio

F/A_{p+s} : fuel to primary plus secondary air ratio

P_{tp} : static tailpipe pressure (psia)

* Data taken on different day with different fuel tank fill from other runs

TABLE I. FLOW DATA OF PRIMARY DATA SET

RUN NR.	t_1	t_2	STACK EXHAUST T_r	T_b	T_w	$\bar{Q}_r/\bar{Q}_b$	d_{32}	SEM DIAM.	ENGINE EXHAST T_r	T_b	$\bar{Q}_r/\bar{Q}_b$	d_{32}
1	1300	1200	42	23	53	.59	.11/.16	.11-.15	90	80	.45	--
2*	1400	1300	55	30	68	.50	--	.08-.09	94	90	.60	.10/.17
3	1300	1200	45	29	59	.65	.08/.20	.09-.14	93	91	.75	.03/.25
4	1400	1300	41	26	67	.66	.07/.21	--	95	--	--	--
5	1300	1150	38	21	51	.62	.09/.18	--	89	76	.42	--
6	1350	1250	37	21	58	.64	.08/.19	.12-.15	91	79	.42	--

LEGEND

t_1 : combustor exit temperature (Deg. F.)

t_2 : nozzle exhaust temperature (Deg. F.)

T_r : percent transmittance of red (6328Å) laser beam

T_b : percent transmittance of blue (4880Å) laser beam

T_w : percent transmittance of white light as measured by transmissometer

$\bar{Q}_r/\bar{Q}_b$: ratio of red to blue mean extinction coefficients calculated from $(\ln T_r)/(\ln T_b)$

d_{32} : mean particle diameter from best available curve, i.e., Figure 14 (microns)

SEM DIAM: range of particle diameters as measured from scanning electron microscope (SEM) (microns)

-- : data not available

* Data taken on different day with different fuel tank fill from other runs

TABLE II. TRANSMITTANCE DATA OF PRIMARY DATA SET

RUN NR.	DESCRIPTION	$\dot{m}_f$	$\dot{m}_p$	$\dot{m}_s$	$\dot{m}_{e_{AIR}}$	$\dot{m}_{t_{AIR}}$	AUG. RATIO	F/A_p	F/A_{p+s}	P_{tp}
7	JP-4 W/O	.0148	.196	.166	1.05	5.82	4.5	.076	.041	24.8
8	ADDITIVES	.0148	.196	.166	1.05	5.82	4.5	.076	.041	24.8
9	JP-4 W/ .2%	.0147	.175	.195	1.01	5.62	4.6	.084	.040	23.4
10	FERROCENE	.0147	.175	.195	1.01	5.62	4.6	.084	.040	23.4
11	JP-4 W/O	.0144	.189	.235	1.13	5.49	3.9	.076	.034	24.9
12	ADDITIVES	.0144	.189	.235	1.13	5.49	3.9	.076	.034	24.9
13	JP-4 W/O	.0124	.206	.205	1.12	4.94	3.4	.060	.030	20.8
14	ADDITIVES	.0124	.206	.205	1.12	4.94	3.4	.060	.030	20.8
15	JP-4 W/ .2% FERROCENE	.0124	.206	.199	1.13	5.41	3.8	.060	.031	23.6

LEGEND

See Table I.

TABLE III. FLOW DATA OF SECONDARY DATA SET

RUN NR.	t_1	t_2	STACK EXHAUST T_r	T_b	T_w	$\bar{Q}_r/\bar{Q}_b$	d_{32}	SEM DIAM.	ENGINE EXHAUST T_r	T_b	Q_r/Q_b	d_{32}
7	1172	--	--	--	49	--	--	--	V	V	V	--
8	1460	1350	V	V	63	V	V	--	--	--	--	--
9	1189	--	--	--	50	--	--	--	--	--	--	--
10	1468	1350	V	V	71	V	V	--	94	92	.74	.04/.24
11	1342	--	--	--	62	--	--	--	--	--	--	--
12	1500	1350	V	V	66	V	V	--	92	74	.28	--
13	1250	--	--	--	52	--	--	--	--	--	--	--
14	1290	1200	V	V	51	V	V	--	92	97	2.8	--
15	1280	1200	V	V	56	V	V	--	98	93	.29	--

LEGEND

See Table II

V : Void - data was taken in unreliable operating range of instrumentation.
--: data not taken.

TABLE IV. TRANSMITTANCE DATA OF SECONDARY DATA SET

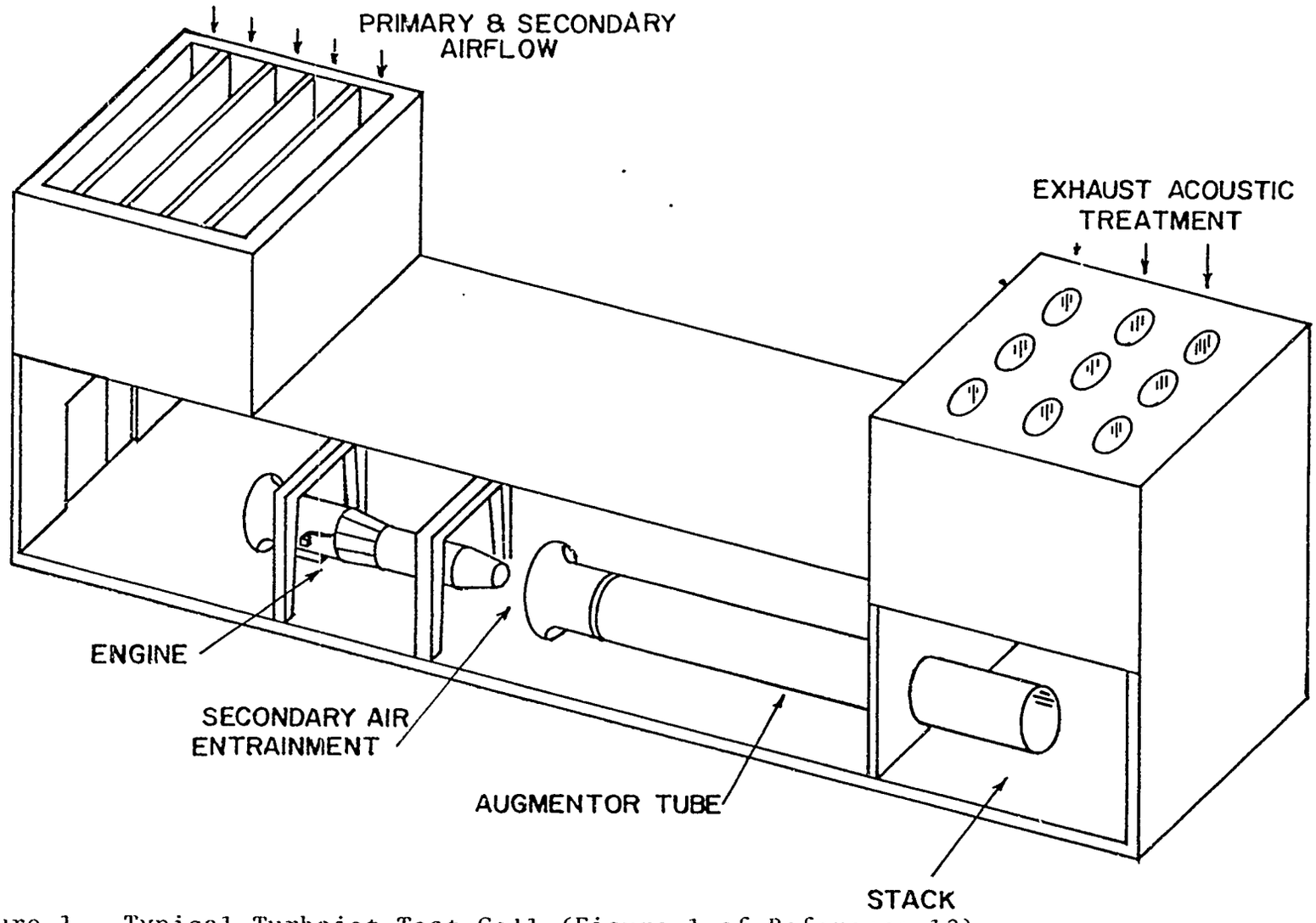

Figure 1. Typical Turbojet Test Cell (Figure 1 of Reference 12)

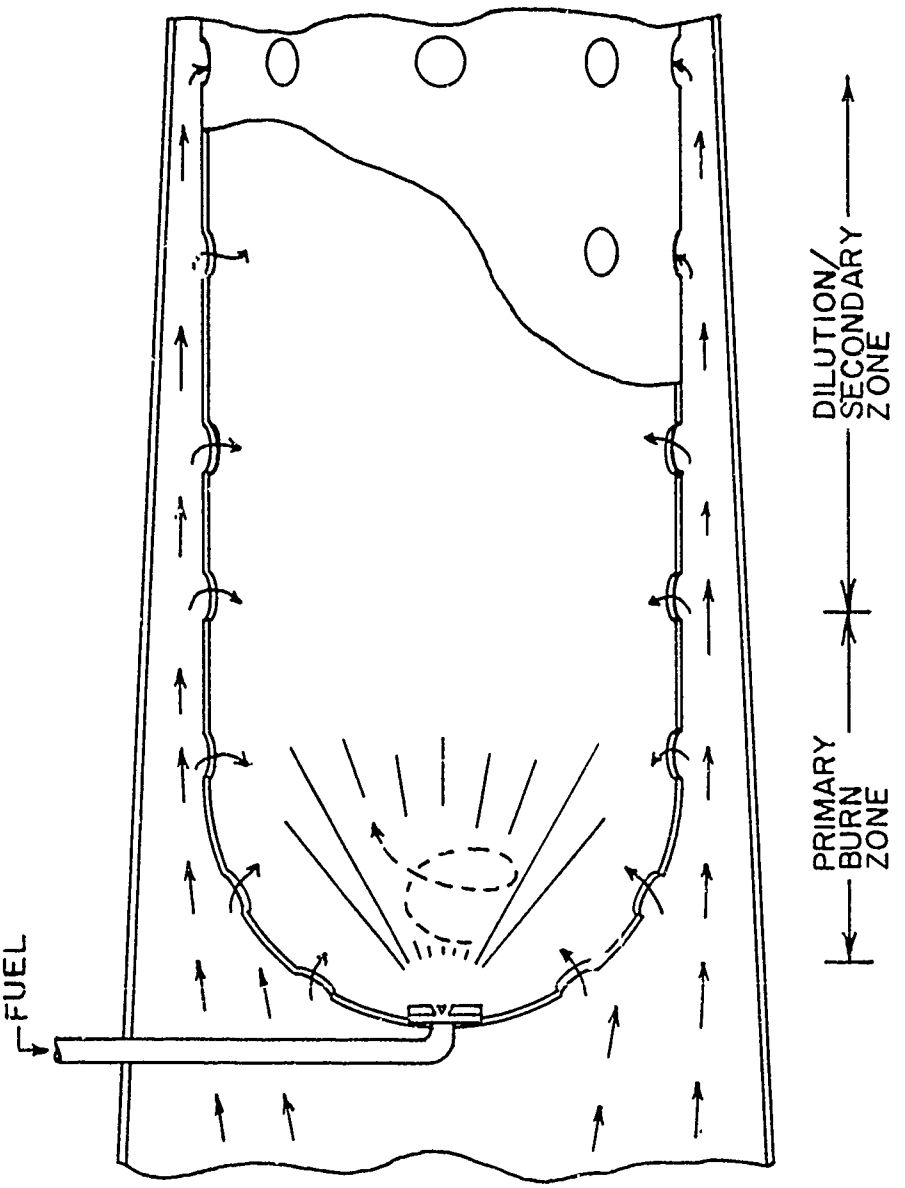

Figure 2. Typical Jet Engine Combustor

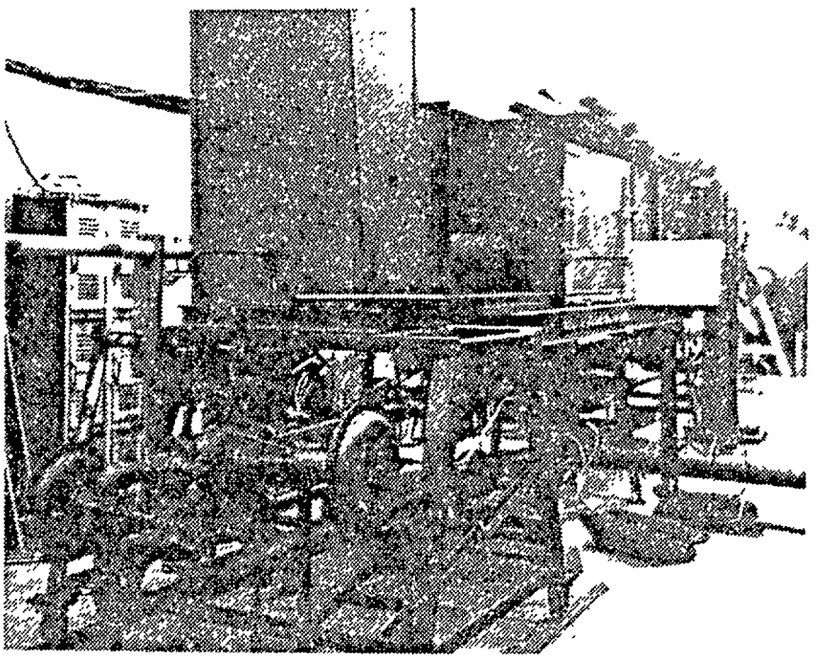

Figure 3

Photograph of Sub-Scale Test Cell

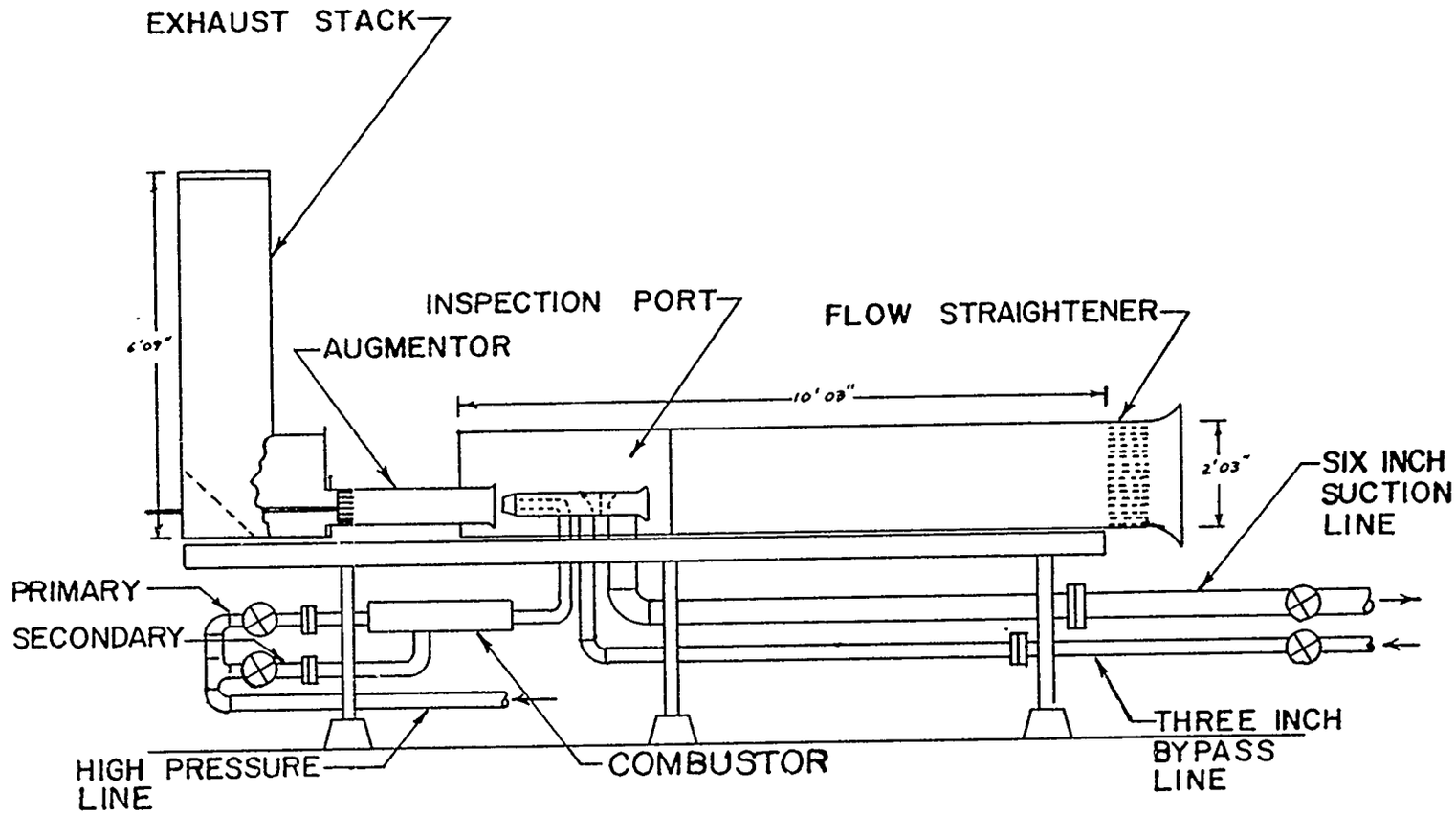

Figure 4. Sub-Scale Test Cell Plumbing

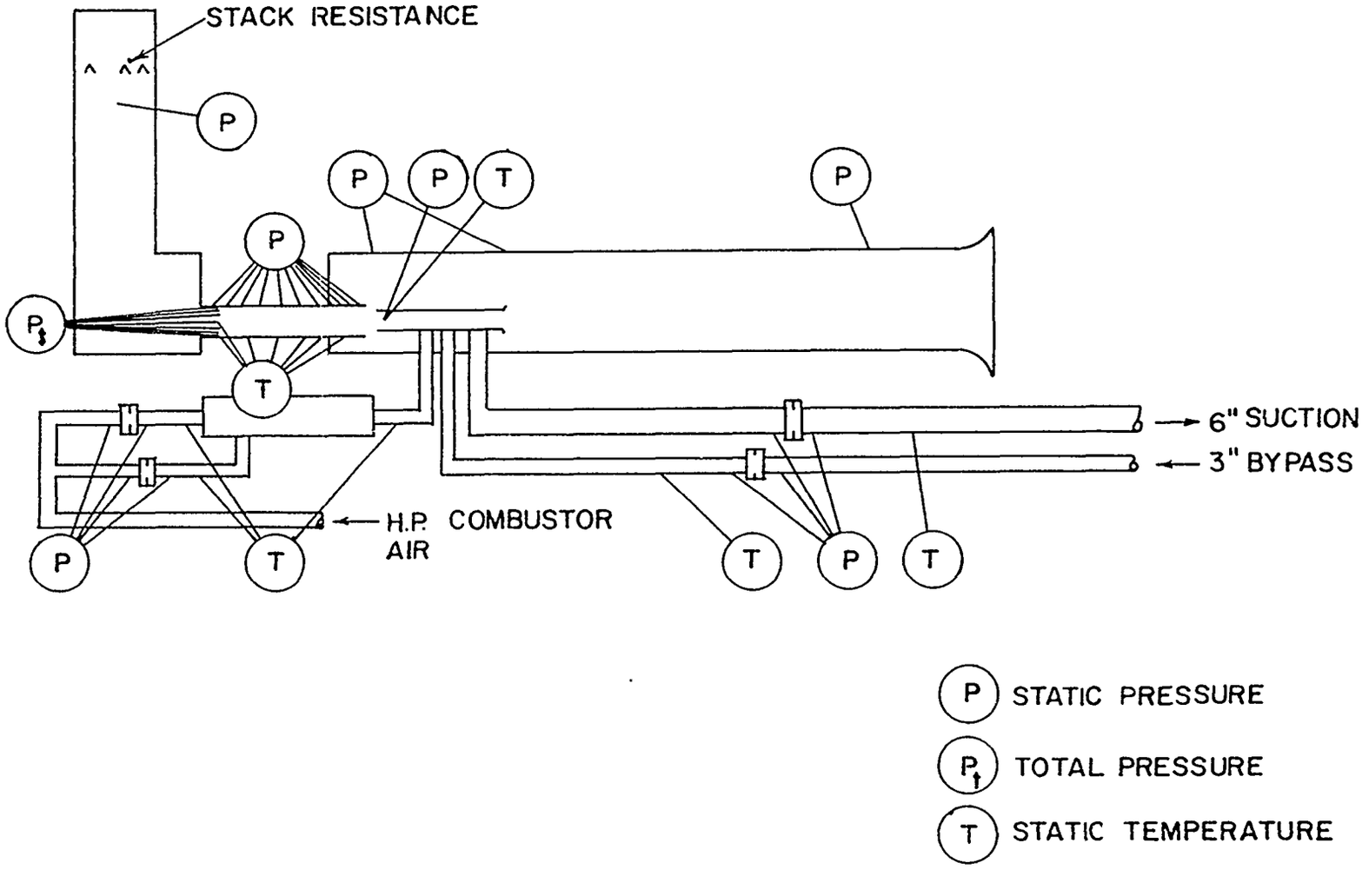

Figure 5. Data Sensor Locations on Sub-Scale Test Cell

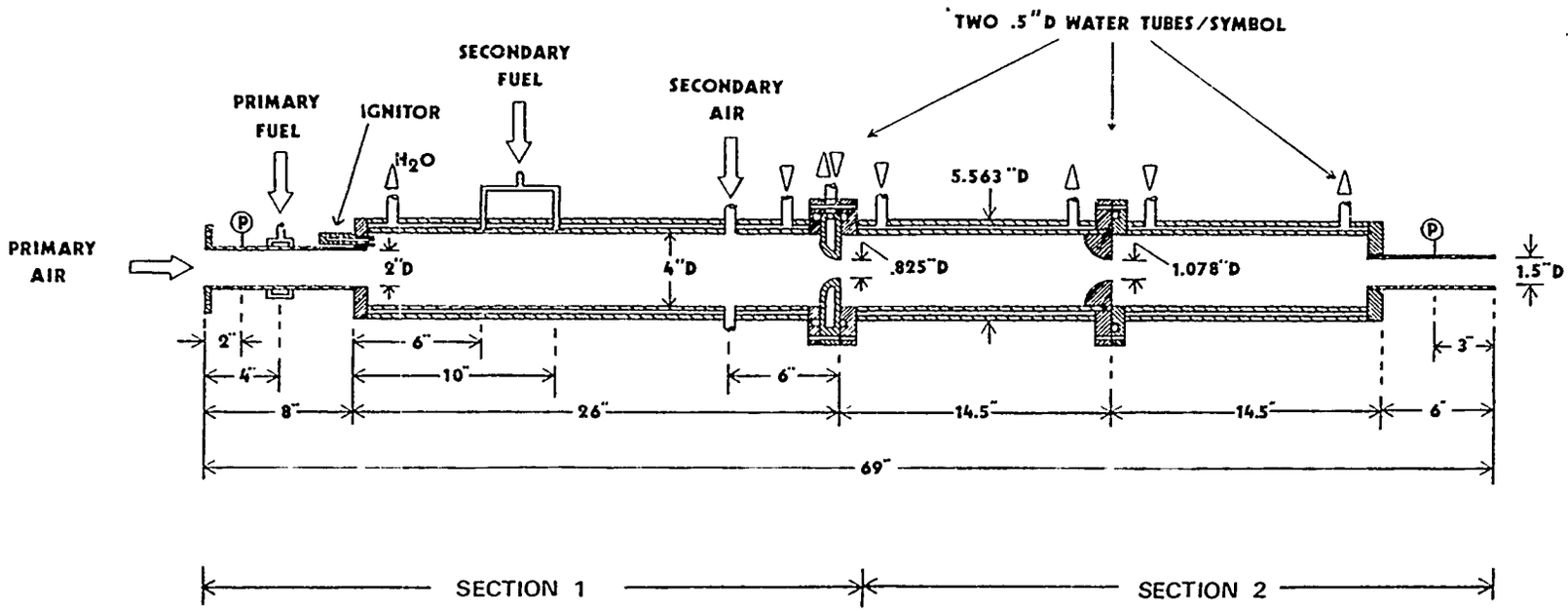

Figure 6. Schematic of Water-Cooled Ramjet Type Dump-Combustor
(Figure 3 of Reference 13)

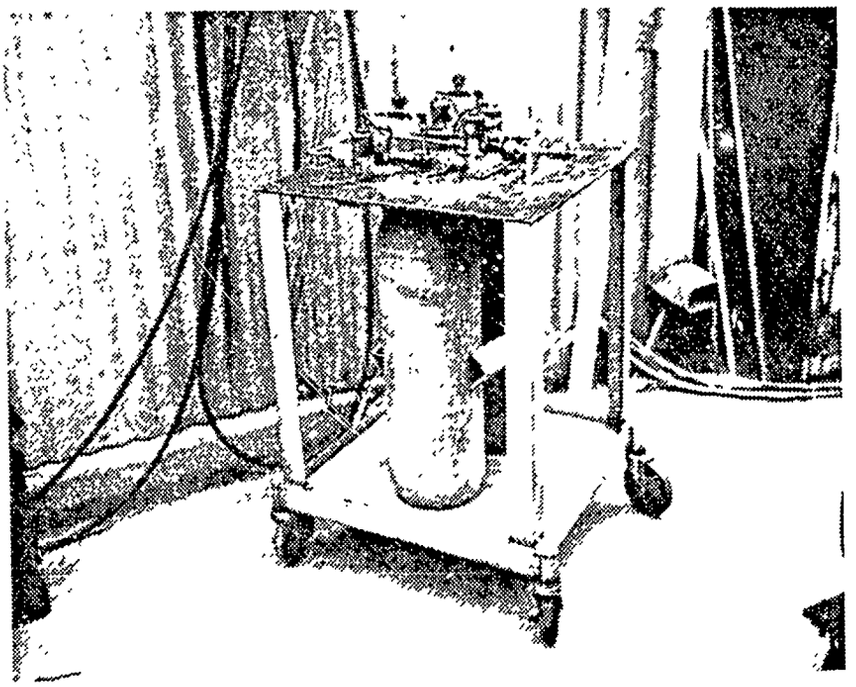

Figure 7
Photograph of Portable Fuel Supply System

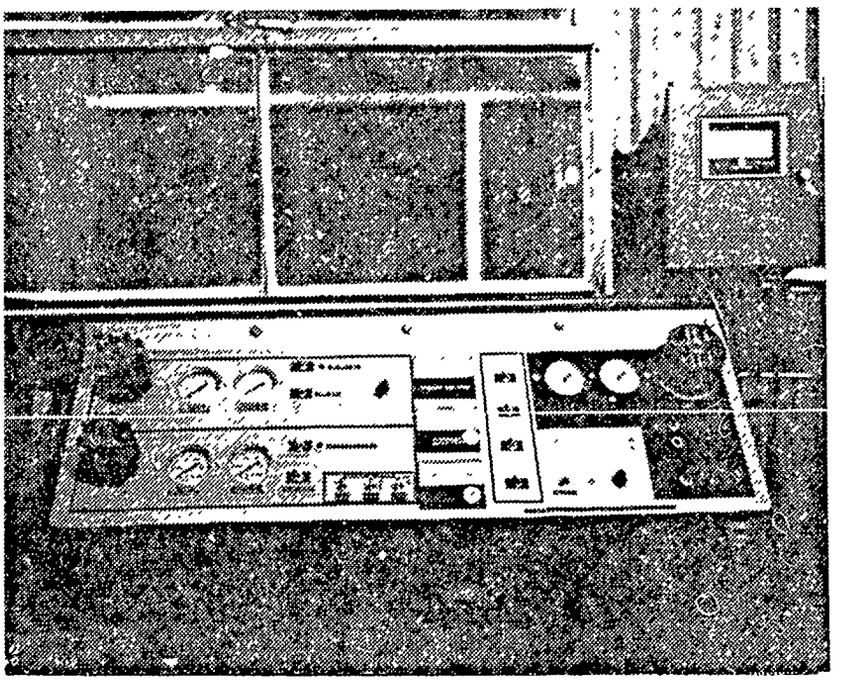

Figure 8
Photograph of Fuel Control Panel and
Transmissometer Signal Conditioner/Display Unit

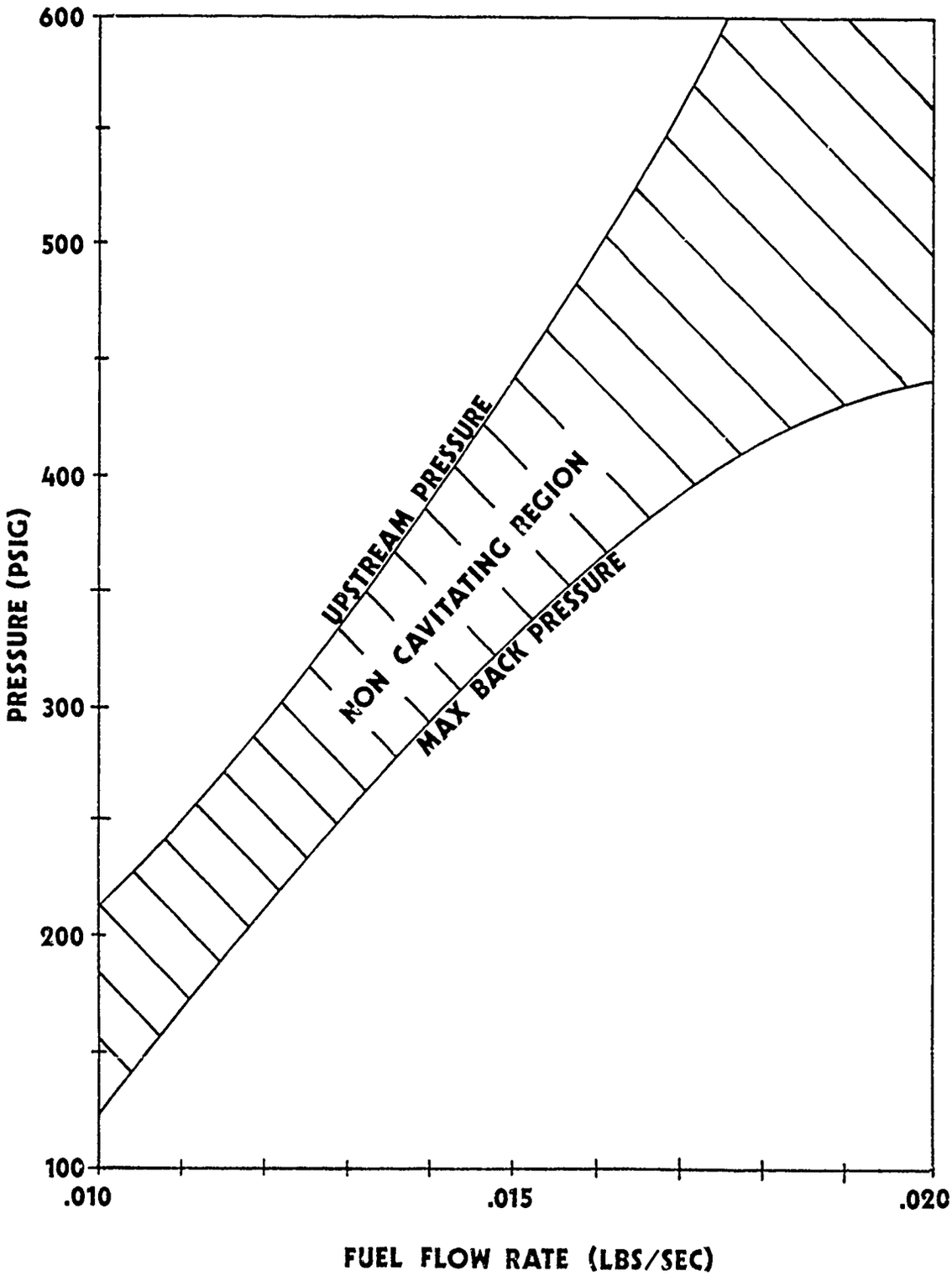

Figure 9. Cavitating Venturi Pressure vs. Flow Rate for .016-Inch Diameter Venturi (Figure 7 of Reference 13)

DATE 11/26/79 RUN NUMBER 1.11

LOCAL BAROMETRIC PRESSURE (IN HG) = 29.98

	DP (IN H20)	P (IN HG)	T (DEG. F)	FLOW RATE (LB/S)
6 INCH SUCTION	12.76	29.68	54.93	1.236
3 INCH BY-PASS	67.22	49.34	100.76	.875
MOTOR PRIMARY	182.68	86.32	50.44	.213
MOTOR SECONDARY	133.20	108.33	50.76	.208

TOTAL ENGINE AIR OUT = 1.296 LB/S

AUGMENTOR TUBE MASS FLOW RATE = 5.545 LB/S

AUGMENTOR TUBE TEMP AT RAKE = 63.74 DEG. F

AUGMENTATION RATIO = 3.279

Figure 10. Page 1 of Typical Output Data Sheet

TEST CELL DATA

ALL PRESSURES IN PSIA

1.	APPLIED TRANSDUCER REF. PRESSURE	19.595
2.	ATMOSPHERIC	14.726
3.	6 IN. SUCTION LINE DOWN STREAM	14.119
4.	6 IN. SUCTION LINE UP STREAM	14.580
5.	3 IN. BYPASS AIR DOWN STREAM	21.776
6.	3 IN. BYPASS AIR UP STREAM	24.205
7.	PRIMARY BURNER AIR DOWN STREAM	35.708
8.	PRIMARY BURNER AIR UP STREAM	42.308
9.	SECONDARY BURNER AIR DOWN STREAM	48.267
10.	SECONDARY BURNER AIR UP STREAM	53.080
11.	AUGMENTOR TUBE STATIC PRESSURE AT RAKE, X=60	14.726
12.	AUGMENTOR TUBE RAKE PRESSURES (WALL-TO-WALL)	14.951
13.	" "	15.063
14.	" "	15.131
15.	" "	15.187
16.	" "	15.120
17.	" "	15.052
18.	" "	14.962
19.	FORWARD TUNNEL	14.704
20.	TUNNEL AT ENGINE INLET FACE	14.704
21.	TUNNEL AT NOZZLE FACE	14.704
22.	STACK	14.704
23.	AUGMENTOR TUBE AT X = .25 (NOT RECORDED)	--
24.	" " X = 1.0	14.423
25.	" " X = 3.0	14.411
26.	" " X = 5.0	14.456
27.	" " X = 8.0	14.456
28.	" " X =12.0	14.490
29.	" " X =20.0	14.535
30.	" " X =32.0	14.636
31.	" " X =44.0	14.704
32.	" " X =56.0	14.704
33.	NOZZLE BYPASS	22.215
34.	RECORDED BAROMETRIC PRESSURE	14.726

ALL TEMPERATURES IN DEG. F.

1.	6 IN. SUCTION LINE	54.9
2.	3 IN. BYPASS	100.8
3.	PRIMARY BURNER AIR SUPPLY	50.4
4.	SECONDARY BURNER AIR SUPPLY	50.8
5.	AUGMENTOR TUBE RAKE	63.7
6.	AUGMENTOR TUBE AT X = 8.0	54.0
7.	" " X = 12.0	55.8
8.	" " X = 20.0	57.7
9.	" " X = 32.0	63.3
10.	" " X = 44.0	64.1
11.	" " X = 56.0	66.9
12.	NOZZLE BYPASS	110.4

Figure 11. Page 2 of Typical Output Data Sheet

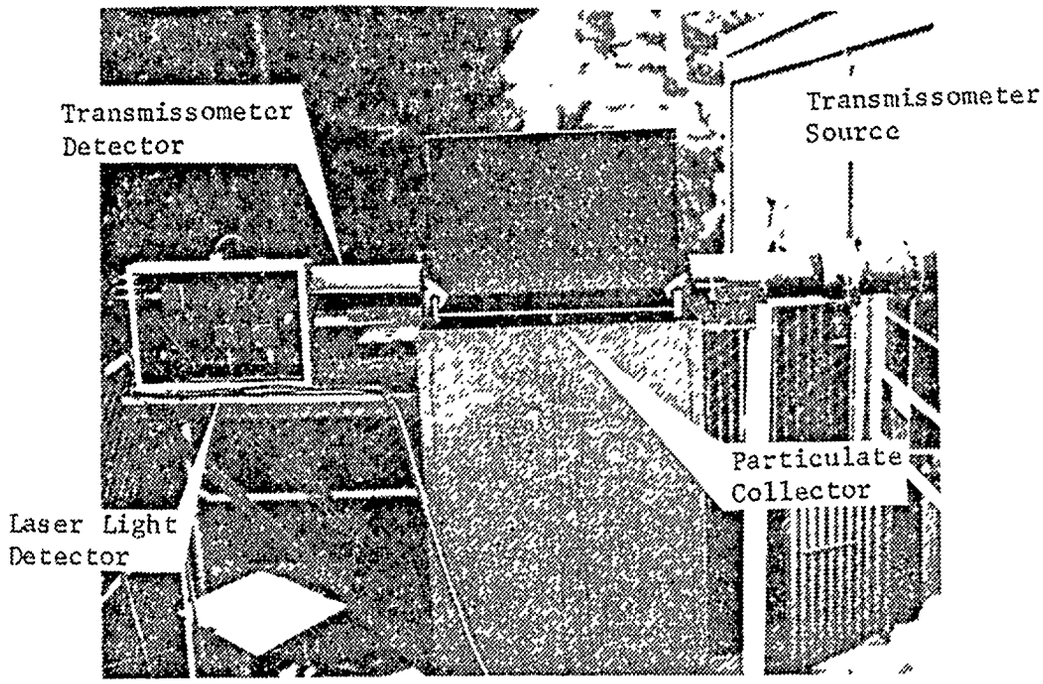

Figure 12

Photograph of Mounted Transmissometer,
Particulate Collector and Stack Detector Unit

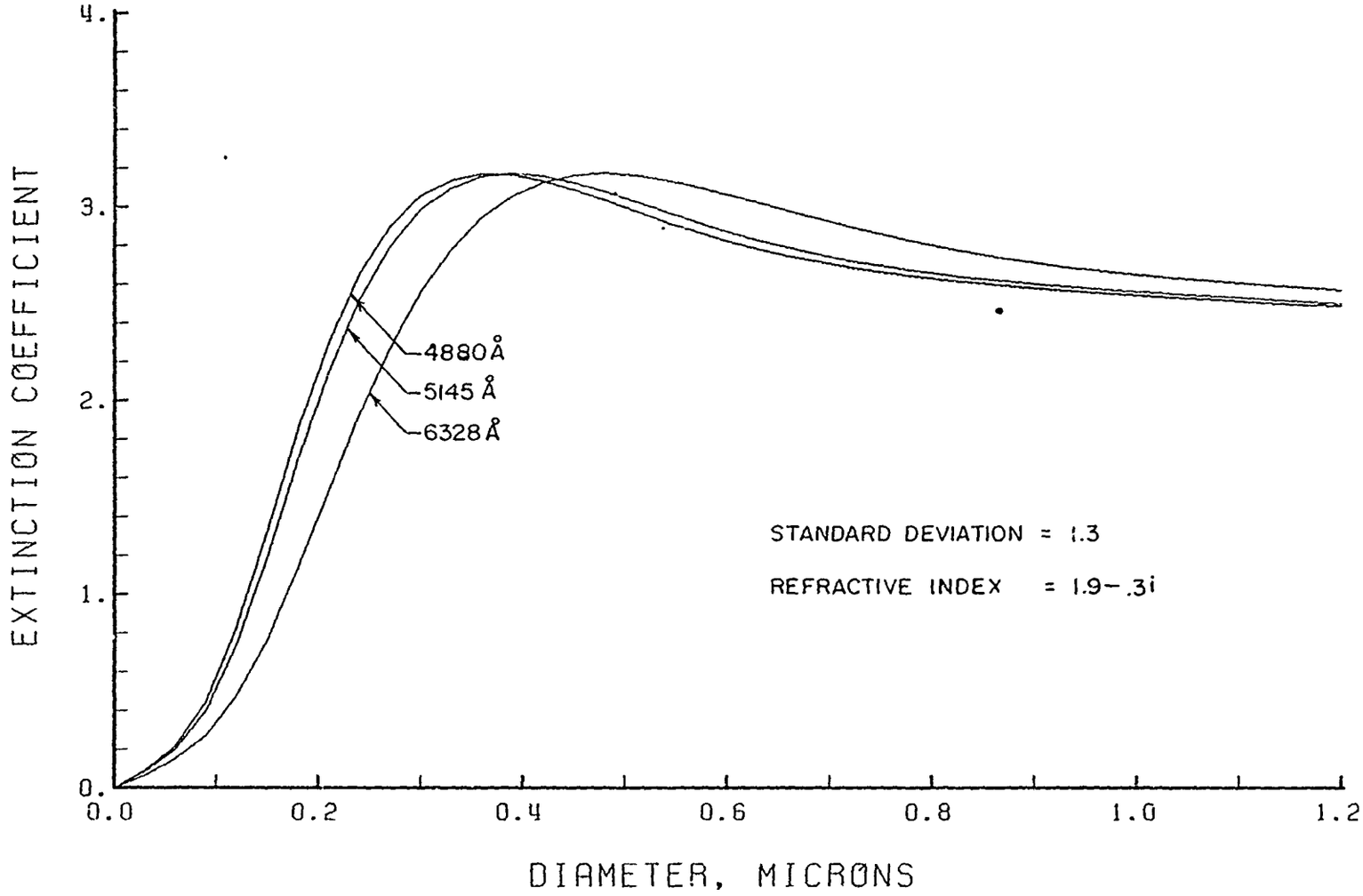

Figure 13. Extinction Coefficient $\bar{Q}$ vs. Mean Particle Diameter

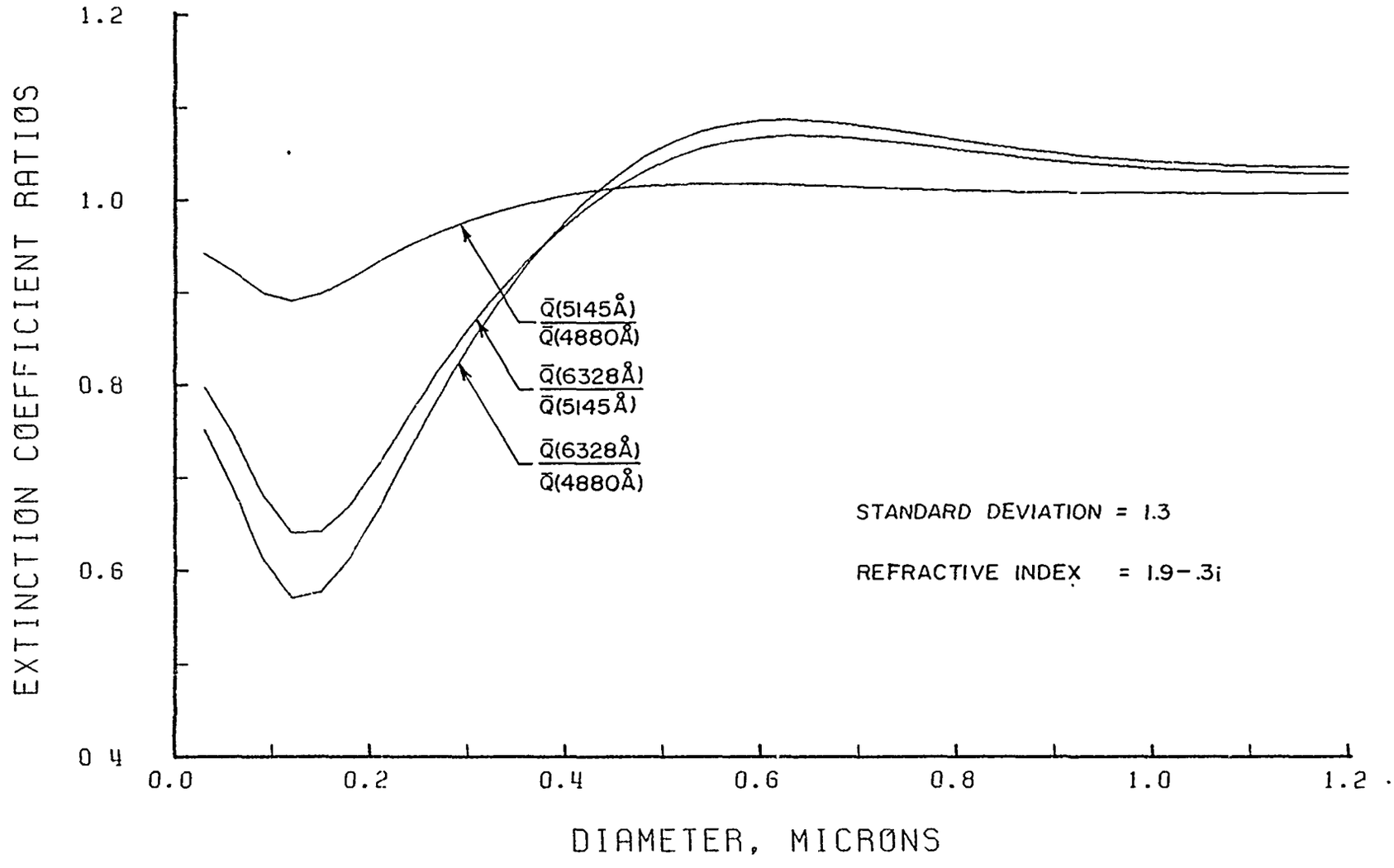

Figure 14. Extinction Coefficient Ratios vs. Mean Particle Diameter

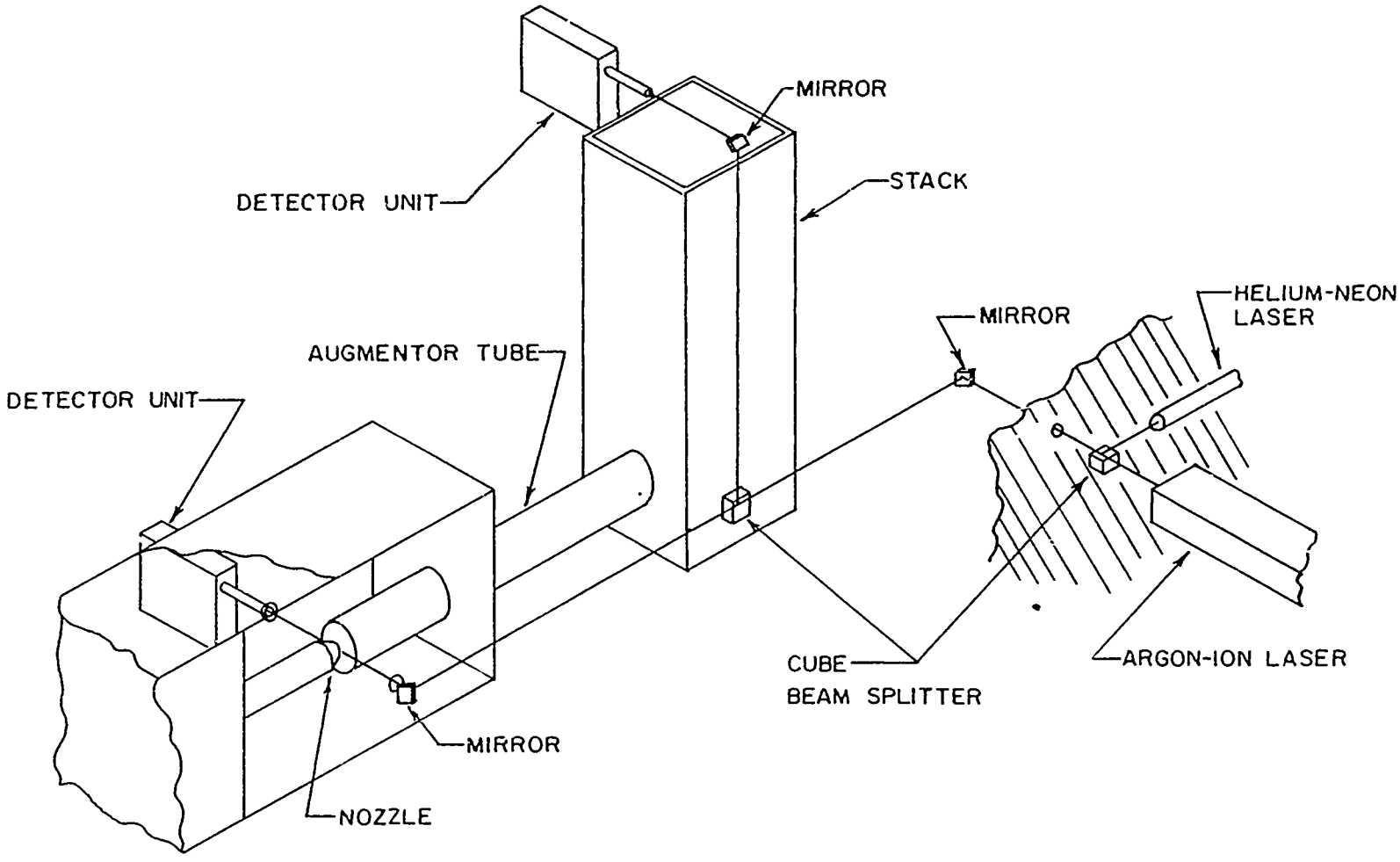

Figure 15. Optical Path of Laser Beams

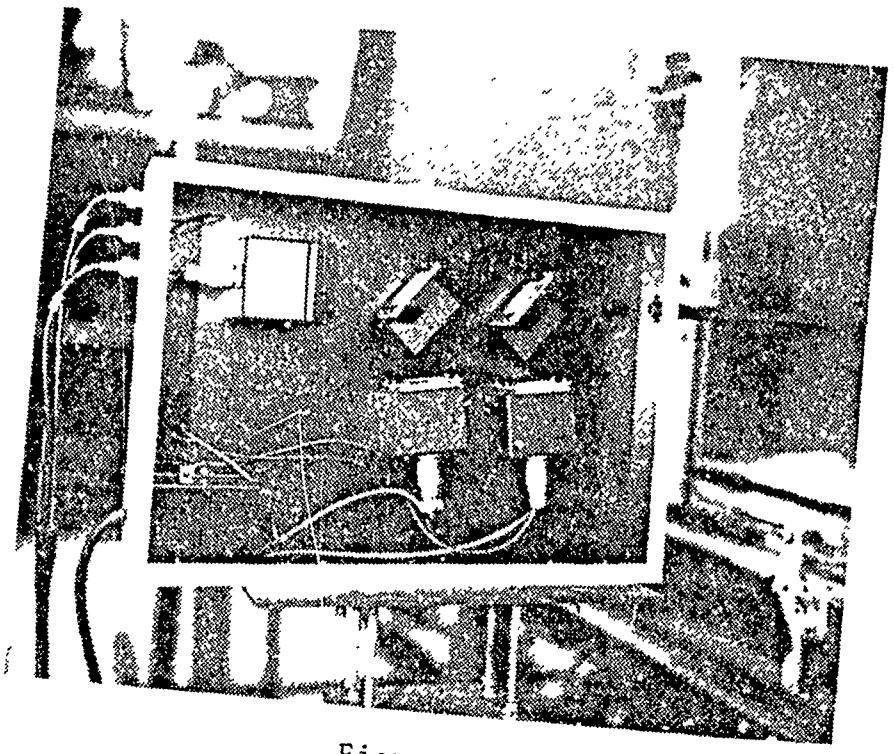

Figure 16
Internal Photograph of Detector Unit

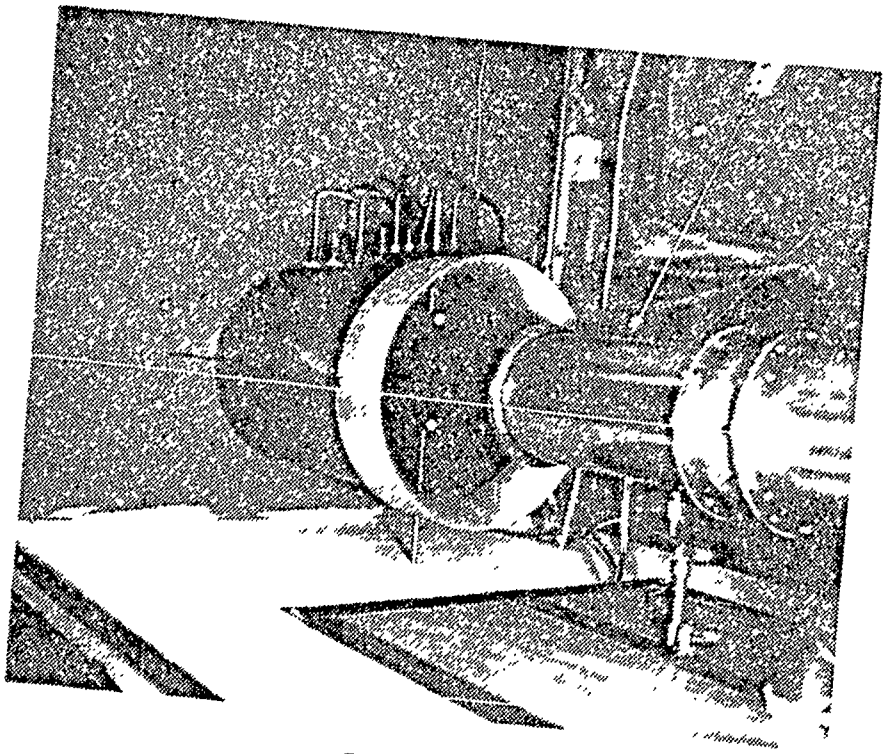

Figure 17
Photograph of Engine Particulate
Collector in the Augmentor Tube

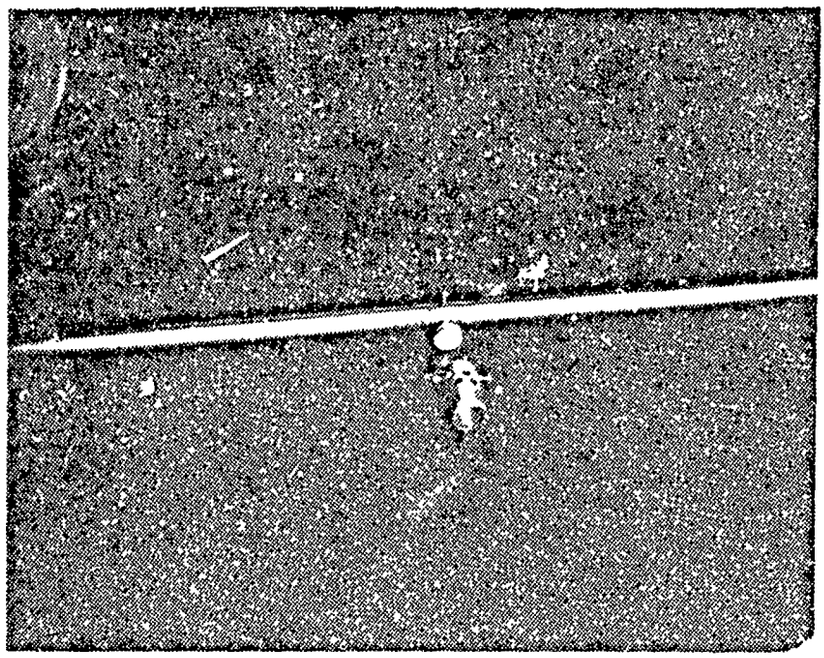

Figure 18
Photograph of Stack Particulate
Collector Arrangement (Unassembled)

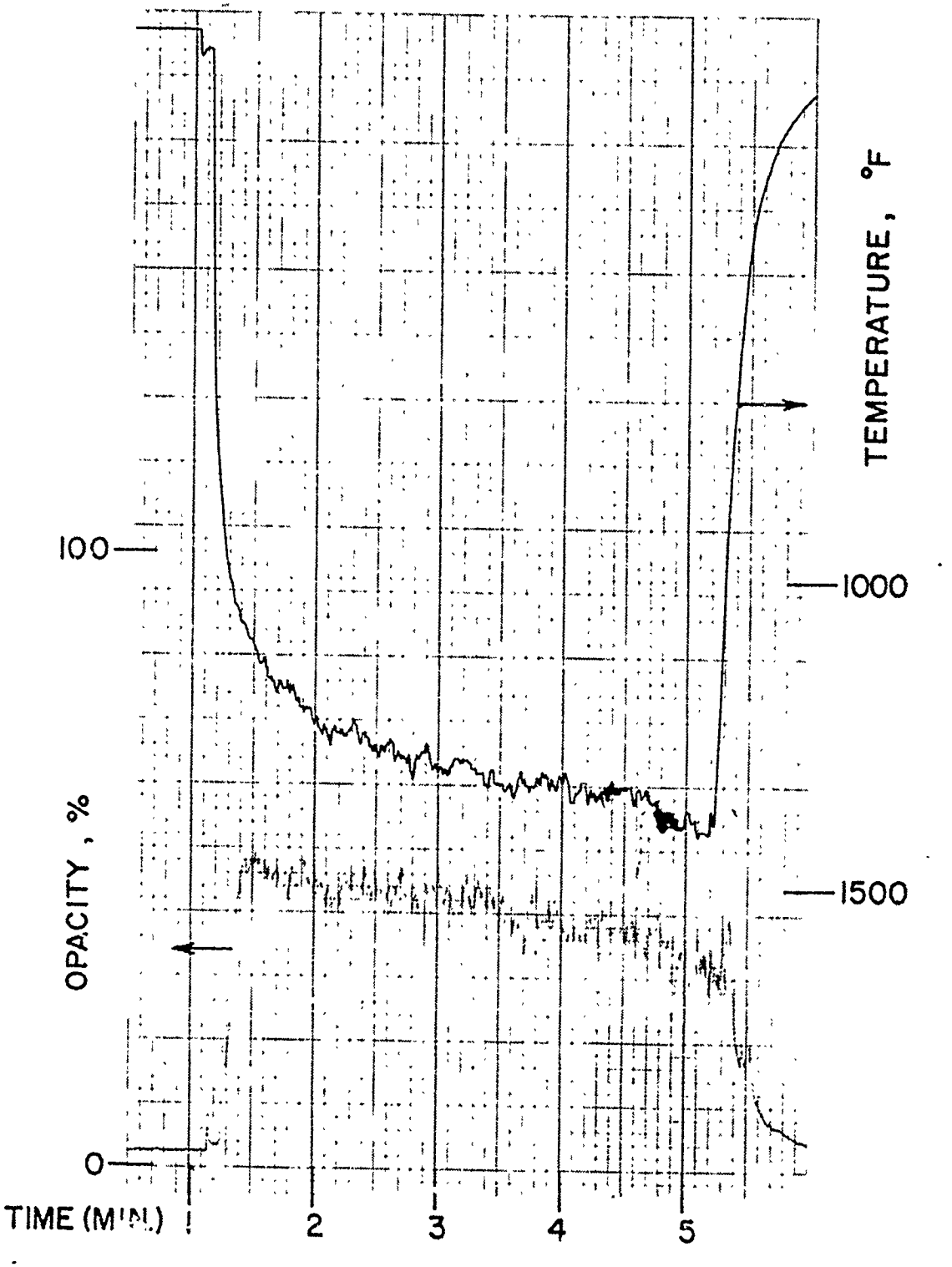

Figure 19

Typical Transmissometer and Combustor Exit Temperature Recording

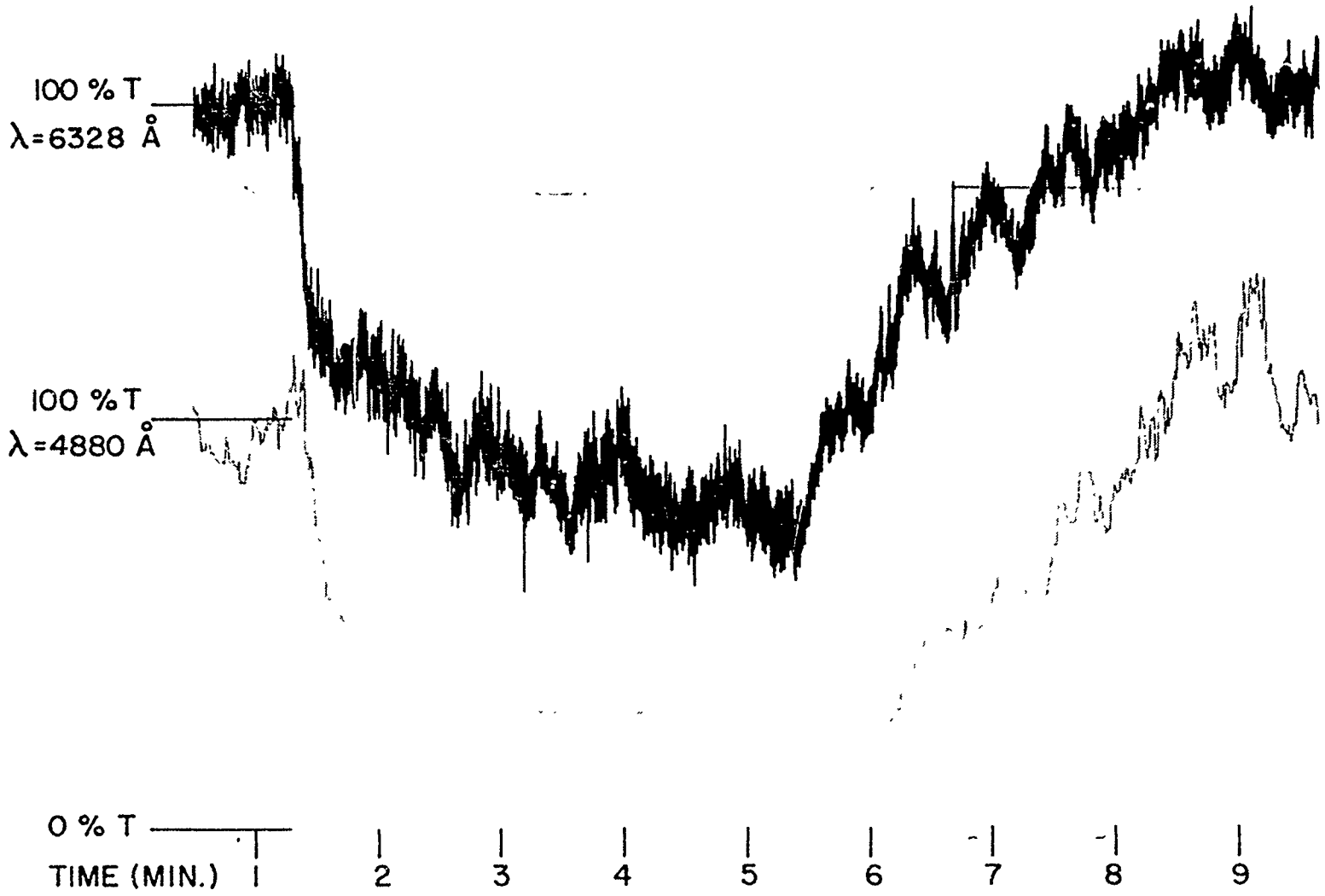

Figure 20. Typical Stack Detector Unit Recording of Blue and Red Laser Transmittance

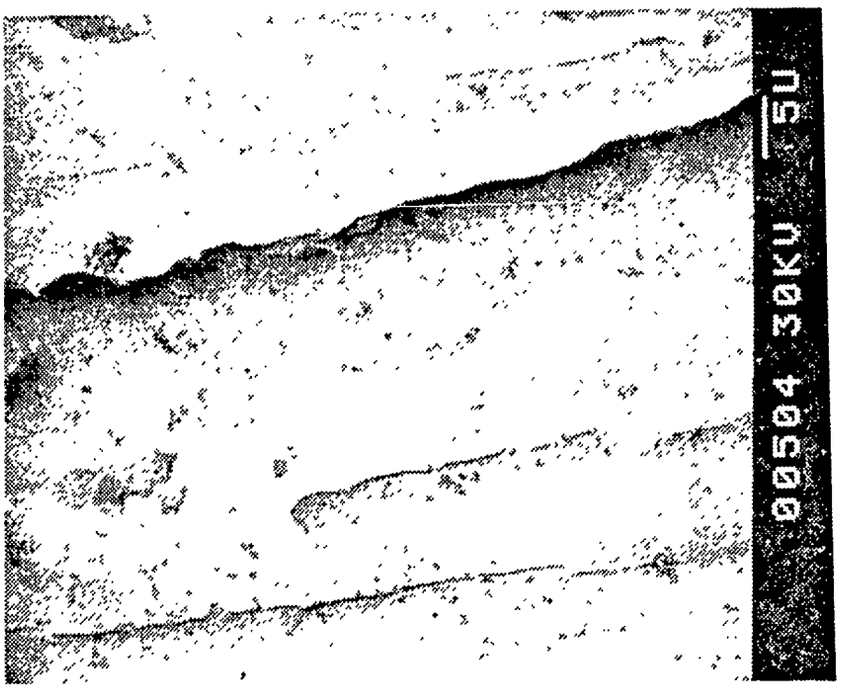

Figure 21

SEM Photograph of Particulates Collected at the Stack. Fuel was JP-4 with Low-Temperature Combustor Exhaust.

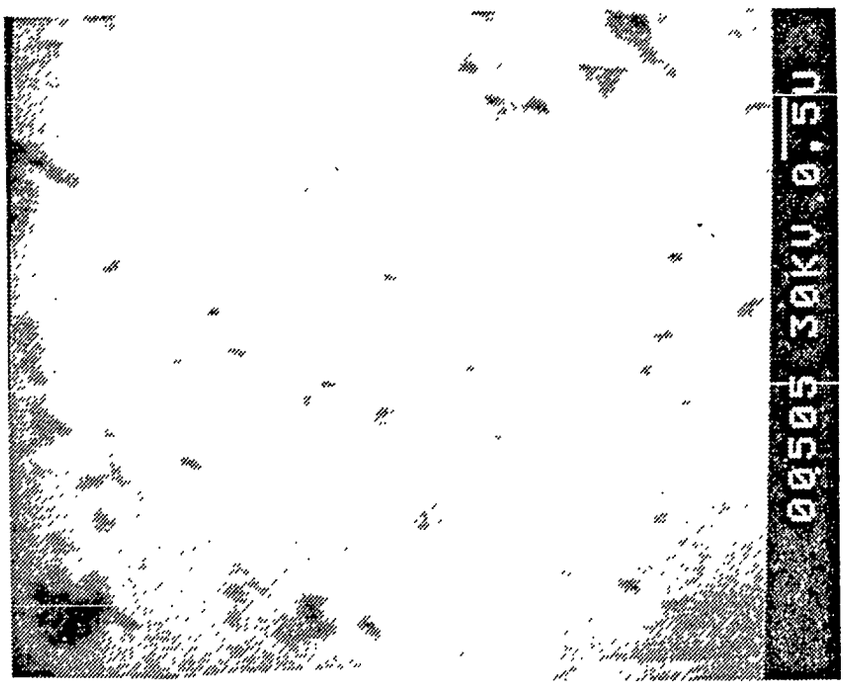

Figure 22

SEM Photograph of Particulates Collected at the Stack. Fuel was JP-4 with Low-Temperature Combustor Exhaust.

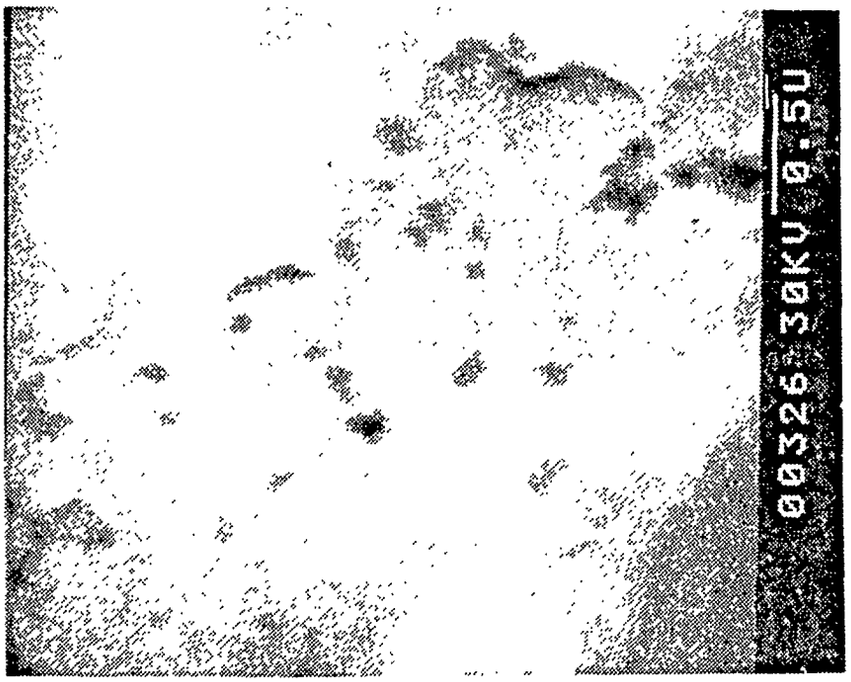

Figure 23

SEM Photograph of Particulates Collected at the Stack. Fuel was JP-4 with High-Temperature Combustor Exhaust.

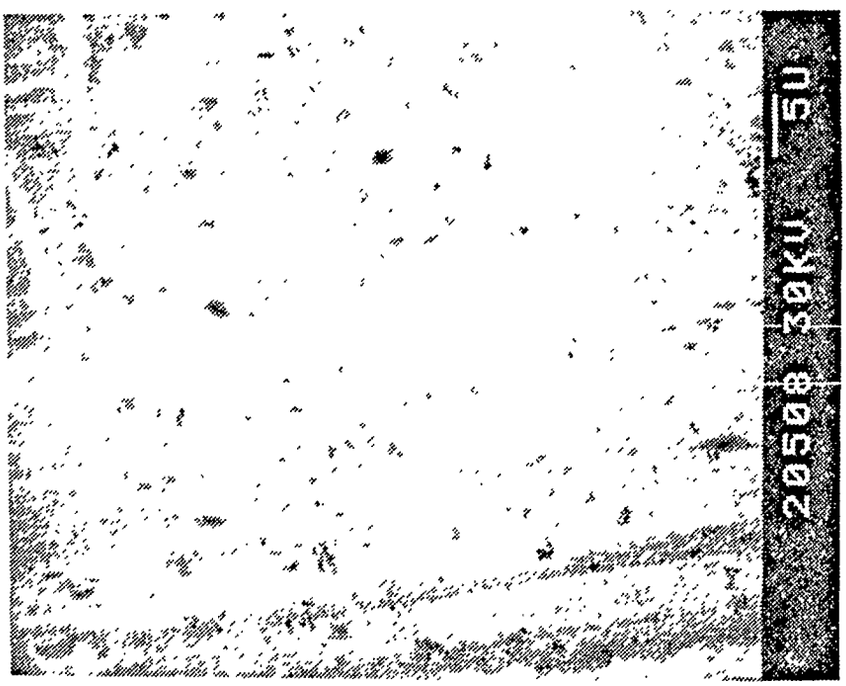

Figure 24. SEM Photograph of Particulates Collected at the Stack. Fuel was JP-4 with 0.2% Ferrocene with Low-Temperature Combustor Exhaust.

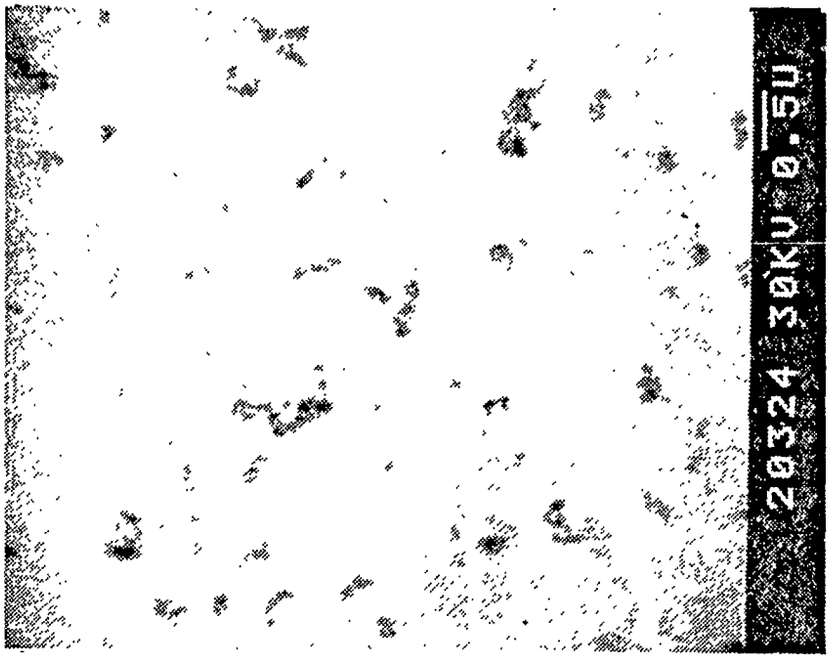

Figure 25. SEM Photograph of Particulates Collected at the Stack. Fuel was JP-4 with 0.2% Ferrocene with Low-Temperature Combustor Exhaust.

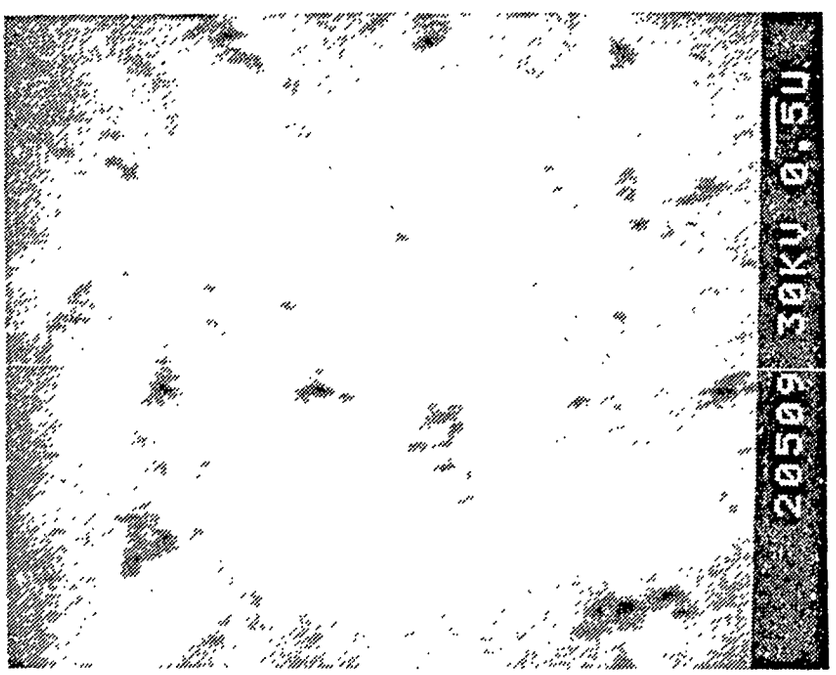

Figure 26. SEM Photograph of Particulates Collected at the Stack. Fuel was JP-4 with 0.2% Ferrocene with Low-Temperature Combustor Exhaust.

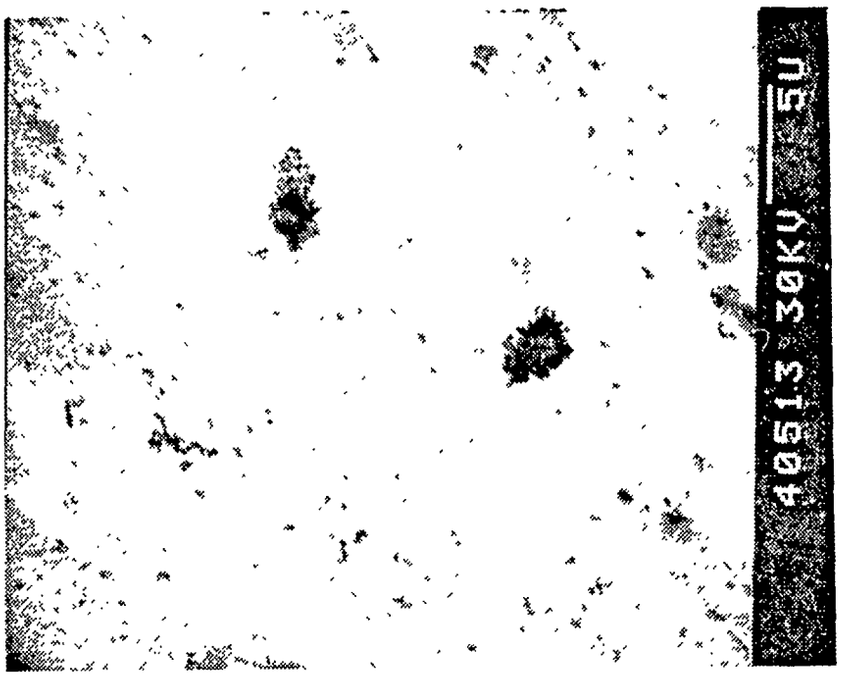

Figure 27. SEM Photograph of Particulates Collected at the Stack. Fuel was JP-4 with 0.2% DGT-2 with High-Temperature Combustor Exhaust.

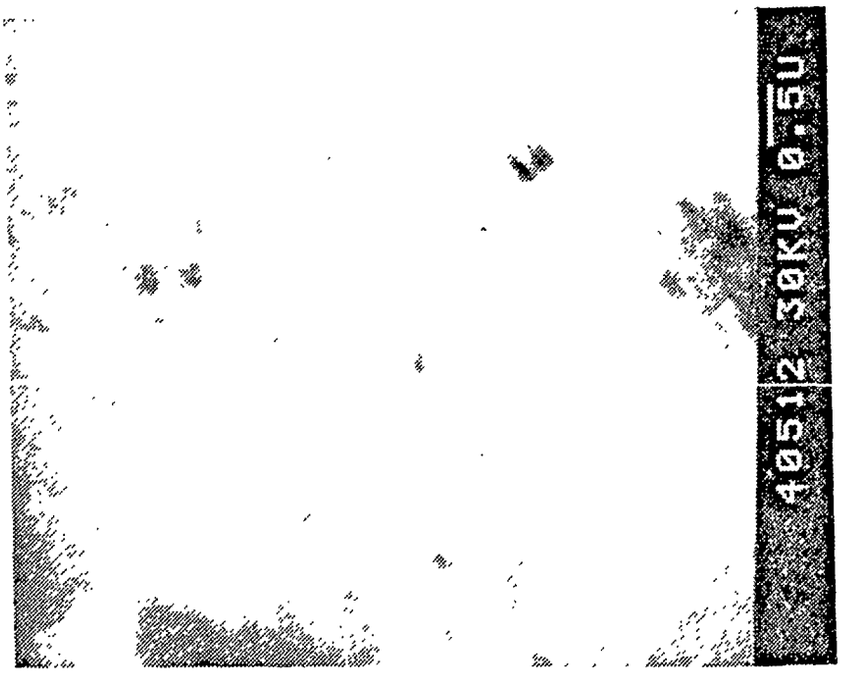

Figure 28. SEM Photograph of Particulates Collected at the Stack. Fuel was JP-4 with 0.2% DGT-2 with High-Temperature Combustor Exhaust.

LIST OF REFERENCES

1. Naval Air Propulsion Center Report NAPC-LR-79-10, Application of Gaseous Emission and Smoke Reduction Technology for Selected Navy Aircraft Engines, by A.D. Bonafede and A. F. Klarman, 2 Apr 1979.

2. People of the State of California versus Department of the Navy, Civil Case No. C-76-0045 WHO, United States District Court for the Northern District of California of January 1976.

3. United Aircraft Research Laboratories, Technical Report No. AFWL-TR-73-18, Analysis of Jet Engine Test Cell Pollution Abatement Methods, by F. L. Robson, A. S. Kesten, R. D. Lessard, May 1973.

4. Naval Environmental Support Service, Report No. AESO 161.1-1-76, Field Evaluation of Instruments for the Determination of Smoke Opacity, September 1976.

5. McDonald, J. E., Visibility Reduction due to Jet-Exhaust Carbon Particles, Institute of Atmospheric Physics, the University of Arizona, Tuscon, Arizona, September 1962.

6. Naval Environmental Protection Support Service, Report No. AESO 111-72-2, Particulate Emissions from J79, J52, J57, TF30, and TF41 Engines during Test Cell Ferrocene Evaluation, February 1977.

7. Naval Air Propulsion Test Center, Evaluation of the Extended Use of Ferrocene for Test Cell Smoke Abatement; Engine and Environmental Test Results, by A. F. Klarman, October 1971.

8. University of California, Berkeley, Size Distribution of Particles Emitted from a Model Combustor, Report No. TS-72-8, by P. J. Pagni and L. Hughes, October 1972.

9. Air Force Engineering and Service Center, Report No. ESL-TR-79-32, Soot Control by Fuel Additives--A Review, by Howard, J. B. and Kausch, W. T., September 1979.

10. Naval Air Propulsion Test Center, Report No. NAPTC-PE-103, Evaluation of Smoke Suppressant Fuel Additives for Jet Engine Test Cell Smoke Abatement, by A. F. Klarman, February 1977.

11. Naval Postgraduate School Report 67NT-77-091, A Sub-Scale Turbojet Test Cell for Evaluation and Analytical Model Validation, by Hewlett, H. W., Hickey, P. J., and Netzer, D. W., September 1977.

12. Hewlett, H. W., Design, Construction and Testing of a Sub-Scale Turbojet Test Cell, MSAE Thesis, Naval Postgraduate School, Monterey, CA, 1977.

13. Charest, J. R., Combustor Design and Operation for a Sub-Scale Turbojet Test Cell, MSAE Thesis, Naval Postgraduate School, Monterey, CA, 1978.

14. The American Society of Mechanical Engineers (ASME) PTC 19.5;4, Flow Measurement, Instruments and Apparatus, United Engineering Center, 345 East 47th, N.Y., 1959.

15. Durst, F., Principles and Practice of Laser-Doppler Anemometry, Academic Press, 1976.

16. Cashdollar, K. L., Lee, C. K., and Singer, J. M., Three-Wavelength Light Transmission Technique to Measure Smoke Particle Size and Concentration, Applied Optics, Volume 18, Number 11, June 1979.

INITIAL DISTRIBUTION LIST

		No. Copies
1.	Defense Technical Information Center Cameron Station Alexandria, Virginia 22314	2
2.	Library, Code 0142 Naval Postgraduate School Monterey, California 93940	2
3.	Department Chairman, Code 67 Department of Aeronautics Naval Postgraduate School Monterey, California 93940	1
4.	Assoc. Professor D. W. Netzer, Code 67 Nt Department of Aeronautics Naval Postgraduate School Monterey, California 93940	2
5.	LCDR Thomas Richard Darnell 10615 Loire Avenue San Diego, California 92131	2